ANALYZING THE ACCURACY OF MAGNETIC RESONANCE IMAGING IN DIAGNOSING OSTEOARTHRITIS THROUGH ITS COMPARISON TO EVALUATIVE DISSECTION OF THE HUMAN CADAVER TIBIOFEMORAL JOINT

by

KATHERINE KENNEDY

A THESIS

Presented to the Department of Human Physiology
and the Robert D. Clark Honors College
in partial fulfillment of the requirements for the degree of
Bachelor of Science

Spring 2022

An Abstract of the Thesis of

Katherine Kennedy for the degree of Bachelor of Science
in the Department of Human Physiology to be taken June 2022

Title: Analyzing the Accuracy of Magnetic Resonance Imaging in Diagnosing Osteoarthritis Through its Comparison to Evaluative Dissection of the Human Cadaver Tibiofemoral Joint

Approved: *Jon Runyeon, Ph.D.*
Primary Thesis Advisor

Osteoarthritis (OA) is the leading cause for chronic disability in the U.S, affecting over 32 million adults nationwide. Although there is no cure for the age-related disease, early detection and diagnosis is crucial in providing individuals with treatment that will improve joint function, health, and overall quality of life. Often said to be the gold standard of OA diagnosis, Magnetic Resonance Imaging (MRI) has been studied for its methodological accuracy through comparing it to other widely used instruments, such as X-rays. However, such imaging methods offer indirect visualization of the pathological condition, whereas analysis of the joint cartilage itself offers a direct way of evaluating the disease. The purpose of this study was to assess MRI effectiveness in the diagnosis of OA through visualization of common pathological features in the knee both indirectly, using MRI, and directly through evaluative dissection of the cadaveric knee joint. It was hypothesized that the observations and measurements drawn from the direct dissection of the joints would convey clearer indications of OA and the true grade of its severity more so than MRI through the minimal pathological evidence picked up indirectly through magnetic

signals. The goal of this research was to assess this "gold standard" of diagnosing OA in hopes of encouraging more research to eventually increase rates of early diagnosis, improve prevention and treatment plans, and move towards a cure for the incurable disease to maintain whole-joint and overall health. Results indicated a disparity between MRI and direct dissection findings through MRI's lack of sensitivity to severity of OA signs, presenting a large problem with the diagnostic tool as severity of the disease takes priority over presence of the disease in approaching its treatment. This would dismiss MRI as the gold standard for OA diagnosis, and may pave the way for future research on discovering new, superior methods for early detection and accurate diagnosis to prevent, treat, and eventually cure the common joint disease.

Acknowledgements

This research would not have been possible if it weren't for the support of my wonderful thesis committee, funding sources, fellow anatomists, team of radiologists, cadaveric donors, and circle of close peers and family members. First, I would like to thank my inspiring thesis advisor and mentor, Senior Director and Professor Jon Runyeon. Despite the trials and tribulations that COVID-19 brought, Professor Runyeon welcomed me into his anatomy lab dissection course before mentoring me in independent research in that very lab. His guidance through dissection and examination of variable anatomic structures, his optimism in completing a never-been-done study utilizing human donors, and his willingness to support me throughout my project enabled me to present this exciting research. I'd also like to thank my second reader and former professor, Dr. Grace Golden who introduced me to knee pathology through her course and supported me with words of advice and encouragement. Dr. Elizabeth Raisanen, the third member of my committee, has supported me for the past four years as my honors advisor. I am undoubtedly thankful for her assistance in the preparation of my thesis and for her check-ins on my progress and mental health throughout the years. Her advice has guided me in this endeavor, and I am very appreciative of her support.

Next, I'd like to thank the donors in the anatomy lab who have donated their bodies for the purpose of helping students grow their knowledge in anatomy and physiology. If it weren't for their generous donations, I would not have grown passionate about anatomy, which inspired me to carry out this research in the first place. I will be referring to my subjects as *donors* rather than *cadavers* in this paper in

acknowledging the significant contributions they made to the University of Oregon, and to this project.

I would also like to show my gratitude for LCNI and two of its facilitators, technician Scott Watrous and director Alison Burggren, who embraced my inquiries regarding the use of their MRI equipment and assisted me in designing protocols and sequencing methods for the scanning segment of my research. I am also grateful for the assistance of EMT Associates in borrowing their gurney for the delicate donor transfer.

I would also like to express my gratitude for UCSD radiologists Dr. Christine Chung and Dr. Aurea Mohana-Borges, who dedicate their time to researching knee and leg tissue using MRI technology. Their assistance in the professional image interpretation of my MRI scans was crucial for my work's integrity and potential implications in today's medicine.

Next, I'd like to thank my fellow anatomy students who carried out some of the knee dissections that aided me in my analyses.

If it weren't for the generous funding awards from UROP and CURE, I would not have been able to use the equipment necessary to complete my research, and I am extremely grateful for their constant support of student research. Lastly, I'd like to thank my friends and family, specifically my mom, for offering their support and encouragement as I completed my intensive research.

Table of Contents

List of Figures

List of Tables

Appendices

INTRODUCTION

Prominently impacting the stability and mobility of joints such as the knee, Osteoarthritis (OA) is defined as the degeneration of joint cartilage as well as the surrounding structures. OA can be accompanied by severe pain, stiffness, and discomfort, and its early diagnosis not only prevents some of these effects, but also diminishes the further degradation that can only be later treated by invasive, surgical methods such as total knee replacements. The process of diagnosing OA isn't exactly clear-cut; in fact, physicians often diagnose it based solely on the conclusions drawn from quick physical assessments. For complex cases, further testing needs to be performed, and the tool physicians often utilize is imaging. While X-rays don't actually capture images of cartilage, they are useful in analyzing bone pathologies, such as reduced joint space width, osteophyte presence, and subchondral sclerosis which can be tied back to the level of cartilage degeneration that impacted such bony changes. Magnetic Resonance Imaging (MRI), on the other hand, offers images of the cartilage itself as well as the many other impacted soft tissue structures, making it the gold standard in assessing cartilage integrity and diagnosing whole-joint diseases such as OA.

If it weren't for our knees, the largest joints in the human body, we wouldn't be able to carry out many of the functions we do today, from specific movements to simple stability. More importantly, it is the articular cartilage that surrounds the knee that gives it the ability to carry out such vital tasks. The decline or degeneration of this cartilage leads to the dysfunction of the joint and the decline in these everyday tasks, bringing about injury, swelling, and pain, often followed by invasive treatment methods.

Unfortunately, there is no cure. Recognizing what makes up our hardworking joint and why knee health is important is crucial in evaluating the eventual diagnosis of OA.

BACKGROUND

The Knee

The knee is the joint that connects the lower leg to the upper leg. Consisting of three bones: the patella (kneecap), tibia (lower leg bone), and femur (thigh bone), the knee serves as a support system for the body in an upright position. It is also home of the anterior and posterior cruciate ligaments as well as the lateral and medial collateral ligaments, providing stability for the knee and preventing gliding or sliding of the attached bones. Menisci of the knee are responsible for shock absorption, and neighboring muscles and tendons allow for its interconnectivity and range of motion (InformedHealth). Along with identifying all the structures that allow for the knee to perform its critical roles in stability, movement, and shock absorption, we must understand how these structures collectively allow the knee to work before we can discuss the effects of OA on this important joint.

Articular Cartilage

Specifically, articular cartilage coats and lubricates all surfaces of the knee joint to permit low-friction bone movement. It is composed of chondrocytes, fibers, Proteoglycans, and an extracellular matrix, dispersed in three distinctive layers of the cartilage (Brody, 2015).

Key Components

The extracellular matrix or ECM is composed mostly of water and decreases in volume with age. It also contains Proteoglycans, which are proteins that bind water molecules together and allow for the absorption of high-compressive loads (Moore,

2021). Lastly, the ECM contains collagen. Type II collagen is the most abundant collagen in articular cartilage, acting in the ECM to form its cartilaginous framework and provide tensile strength. Cells called Chondrocytes are what create these hardworking fibers and proteoglycan proteins (Moore, 2021).

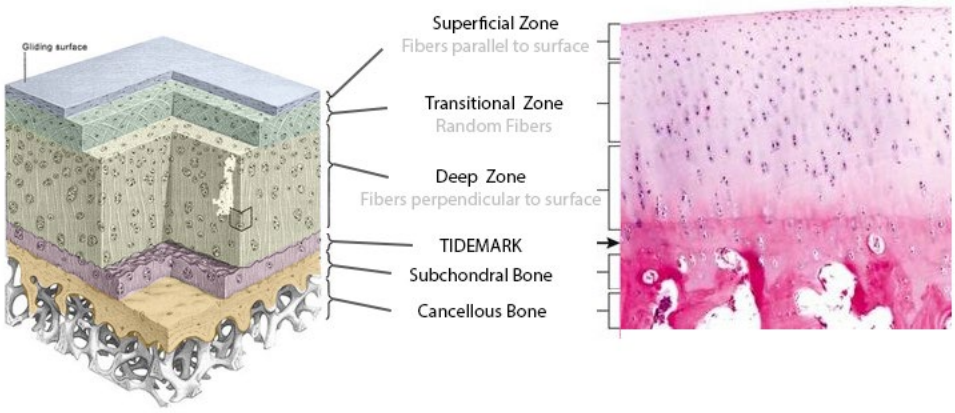

Figure 1: Articular Cartilage Diagram

The left side of the diagram shows an illustrated structure of cartilage. The right image is a histological representation of the cartilage. In both images there are clear zones marked by differences in coloration and components.

Three Zones and the Tidemark

The first outermost layer of the cartilage is known as the Superficial Zone, made up of flat chondrocytes, dense fibers, and very little proteoglycans. Serving as the protective barrier of the deeper layers of cartilage, this zone resists loads. If damage were to occur to this area, the underlying layers would be exposed to shear forces due to naturally occurring inactive chondrocyte activity in this layer, and therefore limited repairability (Brody, 2015). In the next layer called the Intermediate Zone, chondrocytes are much more active, and fibers are even larger and randomized, allowing for more efficient repair if damage were to occur. The Deep Layer lies just above the subchondral bone, consisting of chondrocytes lying vertical to the articular surface, and

fibers lying perpendicular. This layer resists compressive and tensile forces due to a high proteoglycan content (Brody, 2015). Finally, the Tidemark separates the three cartilage layers from the underlying bone. This line of separation is important in understanding how and from where articular cartilage absorbs its nutrients in order to support and serve the knee (Lyons, McClure, McClure & Stoddart, 2005). Above the Tidemark, the cartilage absorbs nutrients from synovial fluid. It also obtains nutrients from below the Tidemark at the subchondral bone. With aging, however, nutrients can no longer come from the bone, eventually giving the cartilage only one source of nutrients and therefore making repair with age much more difficult (Bertrand & Held, 2017). Each layer of cartilage is impacted in some way by OA and will be discussed with the many other observational findings of the knee dissection portion of this research.

Osteoarthritis of the Knee

The knee is the most researched joint affected by OA, and its degeneration is classified under two different categories. Primary OA defines the cartilage degeneration of the knee that occurs due to time and increased risk of development, often associated with aging and gradual wear and tear (Hsu & Siwiec, 2021). Several risks are associated with the development of the disease, ranging from genetic predisposition to obesity and traumatic injury. Several risks, moreover, increase with age, classifying OA as an age-related disease. Secondary OA is usually caused by injury or other underlying factors. While women are more commonly affected by OA than men, there are a number of factors that contribute to the risk of its development, notably being more prevalent with age (Hsu & Siwiec, 2021). In addition to the composition of articular cartilage noted

earlier, it is important to understand the functional system of cartilage. Healthy cartilage will degrade with time, but synthesis will follow to maintain its integrity and function (Hsu & Siwiec, 2021). Matrix metalloproteases, however, become overexpressed in osteoarthritis, disrupting the equilibrium, and resulting in loss of cartilage and proteoglycans (Hsu & Siwiec, 2021). While chondrocytes work hard to repair the system, the degradation overpowers this attempt and leaves the proteoglycans in small numbers, increases the water content, disorganizes the collagen fibers, and destroys the elasticity of articular cartilage. This eventually leads to the cracking and degradation of the cartilage that causes the ultimate erosion of the articular surface and the dysfunction of the rest of the joint (Hsu & Siwiec, 2021).

As emphasized earlier, knee health is crucial in the functional and mechanical aspects of our lives. It is the key player in keeping us mobile, stable, and active (Foret, 2021). Ignorance towards knee pain or carelessness towards knee health can result in joint/cartilage disease such as OA, injury, loss of functionality, severe pain and stiffness, and subsequent invasive treatments, which in turn can affect many more aspects of our lives. With the lack of proper function and mechanics of the knee, many people report an inability to perform daily activities. This leads to immense wage loss due to time off work, and the US has exceeded $100 billion in medical expenses towards OA diagnosis and treatment (Arant, Katz & Loeser, 2021). The proper and early diagnosis of OA is crucial in eliminating such mechanical and financial burdens, but with only the expensive gold-standard diagnostic MRI, it's even more important to evaluate the accuracy of such methods to ensure we are progressing towards a better solution.

Diagnostic Measures of Osteoarthritis

There are many tools and methods used in diagnosing osteoarthritis, ranging from invasive techniques such as surgical arthroscopy to the simplest external examination done directly in your physician's office (Braun & Gold, 2013). Starting from the simpler end of the diagnosis spectrum, physical evaluation focuses on the assessment of pain, swelling, stiffness, and range of motion while also taking the patient's history and age into account. While examining the signs and symptoms of a patient may be useful in identifying cartilage injury, it does not eliminate possible causes of these symptoms aside from OA. Follow-up tests are usually needed to pinpoint joint injury or specific cartilage disease. Blood tests are rare in looking at arthritis, but the removal of synovial fluid may indicate a white blood cell count consistent with OA (Braun & Gold, 2013). Imaging tools such as X-rays, MRIs, and ultrasounds often follow physical evaluation to allow for visualization of the joint in question and present more accurate, complex, and specific diagnoses.

Diagnosis of OA is often done radiographically (using an X-ray), making use of a couple common grading scales specific to this imaging method. Radiographic images offer analysis of OA not through the cartilage itself, but through bony features such as osteophytes or bone spurs, subchondral sclerosis or thickening of the bone, reduced joint space width, and the presence of cysts (Roemer, et. al., 2020). This imaging technique, however, is not sensitive to change over time and does not scan the soft tissue itself. The joint space width that is the focus of OA diagnosis under radiography can also be impacted by other factors aside from OA, offering another limitation in this method of diagnosis.

The next most common diagnostic tool of OA, which will be the focus of this research, is MRI or Magnetic Resonance Imaging. MRIs have the ability to scan both the bony features and the soft tissue of the knee joint, including the cartilage, making it a valuable and common method of diagnosing the whole-joint disease of OA. Its three-dimensional nature allows for overall assessment of tissue dimensions (Roemer, et. al., 2020). Analyzing cartilage thickness allows for a more direct method of testing for cartilage degeneration and OA. Another benefit to this method is its ability to assess the whole joint, enabling researchers and clinicians to take the entire knee into account when examining for OA, as it is a whole-joint disease (Kothari & Peterfy, 2006). Its role in cross-sectional and longitudinal studies and highly progressive visualization allows for the inspection of structures important to the functional integrity of the joint (Kothari & Peterfy, 2006). The debate surrounding the effectiveness of MRI in the diagnosis of OA, however, remains prevalent.

LITERATURE ANALYSIS

While MRI scanning serves as a more complex imaging strategy in clinical testing of cartilage disease, some researchers question its accuracy and purpose in diagnosing osteoarthritis. In a knee loading study that uses MRI in the assessment of tissue lesions and injuries stemming from OA, researcher Eric Y. Chang and his colleagues found challenges in the use of such a complex method. While the MRI allowed them to accurately analyze longitudinal changes in cartilage morphology, they found that only the most superficial of structures within the articular cartilage could be analyzed due to their long length of T2s (Chang, Du & Jerban, 2020). This would mean that deeper structures that are crucial to the joint's integrity would not be visualized as clearly, such as the menisci, ligaments, and the bone (Chang, Du & Jerban, 2020). Other researchers also lack interest in using MRI for OA diagnosis. For end-stage OA specifically, it was deemed unnecessary to use such a complex imaging tool when there is enough clinical and radiographic evidence suggesting that OA is clearly evident (Sherman, et. al., 2018). In a 2020 article comparing the accuracy of MRI to radiography and arthroscopy, it was found that MRI seemed to under-diagnose patients with previous Outterbridge grades of a higher level (Munoz-Garcia, et. al., 2020). Lastly, economic costs of MRIs are 10 times that of radiographs and have been found in more studies to under-diagnose OA (Munoz-Garcia, et. al., 2020).

On the other side of this debate are researchers who have found that the use of MRI in diagnosing OA is most accurate. Assistant Professor of Radiology Daichi Hayashi and his collaborators compared MRI effectiveness to that of radiography, highlighting the limitations that X-rays pose when imaging cartilage. In contrast to

radiography, MRI offers early-detection of pathological features that may indicate future joint collapse (Hayashi, Roemer & Guermazi, 2019). Its ability to display features relevant for longitudinal structural changes is crucial in furthering research on OA prevention and clinical trials; but the question remains: Is MRI a useful and accurate imaging technique in the diagnosis of osteoarthritis? According to a 2019 systematic review, researchers found that MRIs showed conclusive signs of OA in otherwise asymptomatic and uninjured knees (Culvenor, et. al., 2020). The high prevalence of OA found in these healthy individuals suggests that long-term structural changes need to be acknowledged throughout the lifespan, through the use of MRI. Other researchers advocated for the use of MRI after scanning the knee for meniscus tears of several subjects, a sign of high risk for OA, and discovering the high sensitivity and specificity of MRI (Ahmed, et. al., 2017).

Lastly, researchers have discovered a lack of concordance between radiographic changes and OA symptoms, suggesting that MRI cannot stand alone in the diagnostic process of OA. However, in subjects over 50 years of age, it was found through the analysis of their MRI images alone that they showed features of OA despite there being no radiographic evidence of the disease (Guermazi, et. al., 2012). This is due to the sensitivity of MRI as it detects changes of soft tissue that may align with OA signs. These results may indicate early, pre-radiographic signs of osteoarthritis in the knees, suggesting that the sensitivity of MRI is helpful in diagnosing the earliest stages of OA (Guermazi, et. al., 2012).

While previous research has tested MRI's accuracy in OA imaging by drawing comparisons between MRI and other imaging techniques, this study aims to take a

different approach. As mentioned earlier, imaging offers an indirect viewing of what's in question. So, while comparing two imaging methods may offer the answer to which approach is more effective, it does not answer whether imaging is a reliable form of pathology interpretation in the first place. Using human donors as my subjects, I compared OA analyses from their MRI images to my observations and measurements of the directly dissected knees, allowing me to analyze the effectiveness of MRI in diagnosing OA. My research will rely on dissection, observation, measurement, magnetic imaging, interpretation, analysis, and comparison. I hypothesized that interpretation of the joint directly through dissection will offer staggering signs of OA that could not be seen through MR imaging, suggesting that other diagnostic tools be sought out for early and effective diagnosis since dissection of the knee would not be practical in living patients.

METHODS

Study Design

Both the human anatomy lab and the Lewis Center of Neuroimaging (LCNI) at University of Oregon were utilized in this study. The subject design included the knees of two donor bodies chosen randomly in the anatomy lab, offering four knees in total for imaging, dissection, and analysis; however, only three were compared due to incomplete dissection of one of the knees. The donors' characteristic information was limited to ensure their privacy; however, both donors were around the age of 70 years and between the weights of 100lbs and 120lbs.

First, the two donors were wheeled from the anatomy lab to LCNI using a suitable gurney donated by EMT Associates. Utilizing the MRI equipment available at LCNI, the donors' knees were scanned using four sequencing methods to ensure proper visualization of bony and soft tissue structures. MRI images were sent to UCSD radiologists Dr. Christine Chung and Dr. Aurea Mohana-Borges for interpretation and analysis surrounding OA pathology.

For the next part of the study, three of the four knees were dissected with the assistance of anatomy students studying in the dissection section. Careful dissection plans were drawn out and followed in reflecting the patellar tendon to directly visualize the knee joint and its surrounding tissues. Following dissection, the four knees were directly analyzed for pathological signs of OA. Lastly, analyses from the dissections were compared to the MRI findings and interpretations to assess the effectiveness of MRI in diagnosing OA.

MRI Acquisition

The first donor, Subject 1, was wheeled to LCNI using the previously described gurney, before being transferred onto the non-ferromagnetic gurney present in the facility. Subject 1 was then carefully positioned into the MRI bore to ensure that their knee was sitting properly inside the knee coil for scanning. Subject 1 was also wrapped securely in leak-proof sheets and bags to maintain cleanliness of the bore and gurney.

The facility operated a Siemens 3T Skyra MRI system. First, a T2-weighted (T2-TSE-TRA) MRI scan was selected for viewing of the right knee in multiple planes, using long repetition times (TR) and long echo times (TE) to enhance the brightness of tissue structures in this specific pulse sequence. Under this sequence, tears would appear bright due to fluid accumulation, making it easy to identify lesions and tears of structures like the menisci. Turbo spin echo (TSE) allowed for fast scanning time and the use of multiple radio sequences per TR.

Next, a SIEMENS sequence (PD-SPACE-ISO) was initiated. This sequence included proton density (PD; short TE) to provide signal-rich images specifically evident in the sagittal plane, using a specialized spin echo sequence (SPACE) for application-optimized contrasts through different flip angles (Hassanzadeh, 2021).

The third sequence used followed another T2-weighted (T2-TSE-SAG) parameter, with a fourth T2 weighted system (T2-ISO) simply incorporating isotropic parameters as well.

These four sequences were then repeated on Subject 1's left knee, before the donor was transferred back to the anatomy lab. Subject 2 was then taken to LCNI and the same transfer and imaging steps were followed for both their right and left knees.

Images for all four knees were transferred to a computer through DICOM-compatible files for optimal viewing and analysis by a team of radiologists.

Evaluative Dissection

For each knee, dissection was carried about by either myself or one of three other fellow anatomists in congruence with their dissection class to ensure appropriate and professional methods for this part of the study. This was completed in a span of 5 weeks. Different plans were followed based on subjective preferences of dissection; however, removal of the skin, fascia, and adipose layer, as well as reflection of the patellar tendon was universal and was crucial in visualizing the underlying structure of the knee.

My dissection began with a longitudinal cut down the posterior aspect of the leg, beginning from the back of the knee to just above the Achilles tendon. I then used dissection scissors, a scalpel, and my hands to remove the skin from the leg, beginning posteriorly and wrapping around the anterior leg. Once the skin layer was removed, the adipose tissue and fascia layer were removed using similar tools. Subject 2 was then flipped into the supine position to shift focus onto the knee join. Dissection was done using common dissection tools available in the anatomy lab, such as scalpels, forceps, probes, dissecting scissors, and more. Integrity of the joint's moisture was maintained using a hydrating spray following a day's dissection, and the donors were stored in adequate conservation tanks to maintain a cool temperature.

MRI Image Interpretation

MRI interpretation was done simultaneously with dissection to allow for ample time for dissection and analysis. The DICOM-compatible images from the four MRI sequences for each knee were sent to UCSD radiologists Dr. Christine Chung and Dr. Aurea Mohana-Borges for analysis. Dr. Mohana-Borges sorted through the hundreds of MRI slices to identify which images presented the clearest for areas in which you'd often see OA features. For example, when assessing cartilage loss or the presence of osteophytes, the areas of interest would include the tibial plateaus, femoral condyles, patella, and trochlea, and when assessing the ligaments, the images would show those four ligaments. Following her narrowing down of the images, Dr. Mohana-Borges used the UCSD MRI Grading Scale of OA to grade the severity and extent of all OA-related pathological signs to then identify the severity and extent of the entirety of the whole-joint disease (Figure 2).

The UCSD OA grading scale groups several pathological features together, such as cartilage degradation with bone marrow edema and osteophyte presence, meniscus effusion with ligament wearing, and synovitis with fat pad inflammation (Figure 2). Cartilaginous and bony OA features were scored based on the extent and severity seen on the patella, trochlea, lateral femoral condyle (LFC), lateral tibial plateau (LTP), medial femoral condyle (MFC), and medial tibial plateau (MTP). Meniscus and ligament extrusions and tears were scored based on the severity seen in the anterior horn of the lateral meniscus (aLM), body of the lateral meniscus (bLM), posterior horn of the lateral meniscus (pLM), anterior horn of the medial meniscus (aMM), body of the medial meniscus (bMM), posterior horn of the medial meniscus (pMM), and on the

severity seen on the anterior cruciate ligament (ACL), posterior cruciate ligament (PCL), medial collateral ligament (MCL), and lateral collateral ligament (LCL). Lastly, synovitis and effusion were scored based on what is identified in the synovium of the joint as well as the three fat pads: pre femoral fat pad, supra patella fat pad, and Hoffa's fat pad.

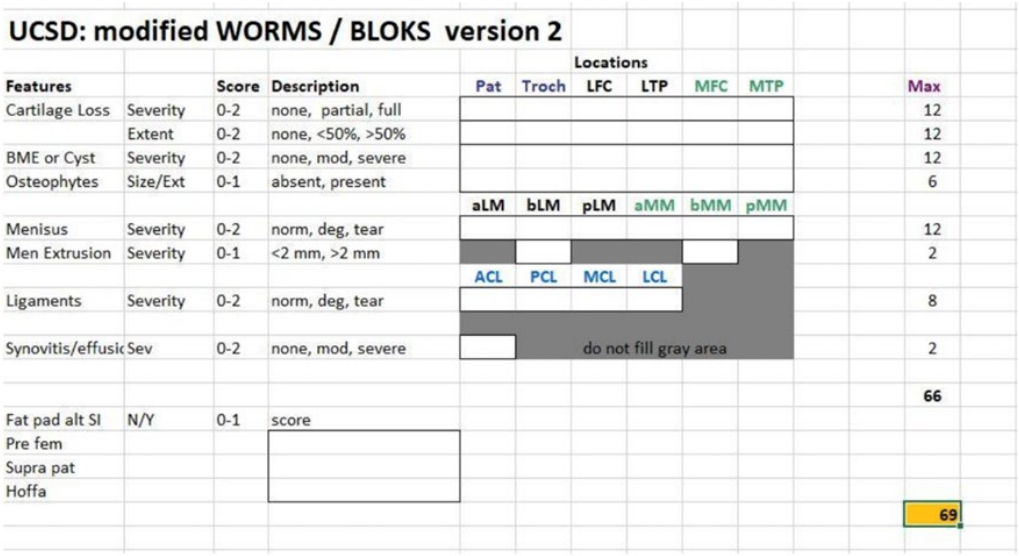

Figure 2: UCSD Grading Scale for OA.

The scale above represents the common grading protocol used at UCSD for analyzing signs of OA through MRI. Pathologies in cartilage, bone, menisci, ligaments, and synovial fluid are all measured using this system, with grades from either 0-1 or 0-2 reflecting the extent and severity of such abnormalities. A score of 69 would signify the highest grade of OA, as shown at the bottom right of the image.

Dissection Analysis

Following dissection, anatomy lab director Jon Runyeon assisted myself in analyzing the knees for OA signs through sight and touch. Each knee was held in a flexed position where we assessed cartilage integrity, bony features, and whatever else presented as an OA-related abnormality. With the possibility of menisci and ligaments being tampered with during dissection, and synovitis and fat pads being unable to be

visualized, only cartilage and bone was analyzed directly. While recording such observations, MRI findings were introduced to where we then compared our dissection findings to the radiologists' discoveries.

Using a modified version of the UCSD MRI Grading Scale of OA, signs discovered through dissection were graded on severity and extent. Again, BME, cysts, synovitis, and often menisci and ligament integrity were too difficult to assess as fluid escape and tampering is common during dissection; however, cartilage degradation, and osteophyte presence were analyzed, graded, and compared to MRI findings. The grading scale was adjusted for this section of the research to focus solely on these two areas (Figure 3).

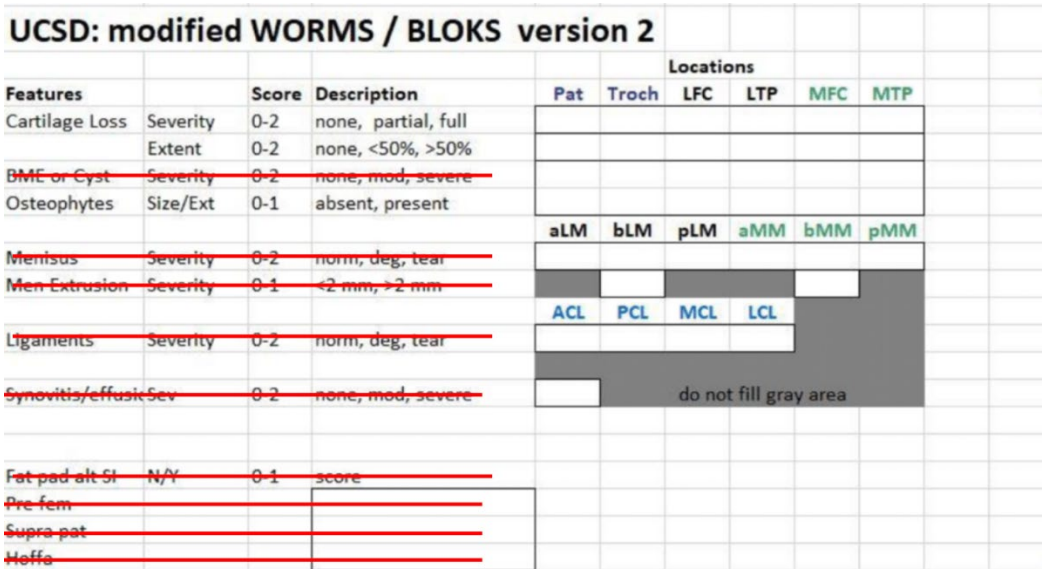

Figure 3: Modified UCSD Grading Scale for OA for Dissection

The scale above represents the common grading protocol used at UCSD for analyzing signs of OA through MRI; however, red lines are shown to cross out the signs that cannot be analyzed through dissection due to fluid escape and tampering. Pathologies in cartilage and bone measured could be measured using this modified system, with grades from either 0-1 or 0-2 reflecting the extent and severity of such abnormalities.

RESULTS

Imaging Results: Subject 1- Right Knee

Following the UCSD grading scale for OA, severity and extent of OA abnormalities were calculated based on key images of OA features identified by Dr. Chung and Dr. Aurea Mohana-Borges (Figures 4 - 5, Appendices A-C). Overall grade of OA within each knee was then calculated by both radiologists. For demonstrative purposes, the MRI of Subject 1, Right Knee will be discussed in full, with images presented, followed by the scores and discussion only of the remaining knees, which images are included in the appendices.

The right knee of Subject 1 presented with several signs of OA, evident in the cartilage, bone, ligaments, menisci, synovium, and fat pads, as seen below (Figure 4, [A] - [F]. Cartilage loss was displayed through abrupt changes in the bright signal that surrounds the knee cartilage, best seen in the PD-T2 sequences. Often blurry or seen as a lack of signal in the image, the cartilage degradation could be seen in the coronal plane of the LFC, MFC, and LTP (Figure 4, [B], [C], [E]). The axial plane shows degradation around the trochlea and patella (Figure 4, [A], [D]).

Bone marrow edema (BME) and cysts were also found in Subject 1's right knee, evident through brighter signaling within the marrow (Figure 5). Edema, or excessive fluid accumulation, can be seen in the patella (Figure 5, [A]). A minor cyst on the LTP is also evident, and while this does not lie on the cartilage surface itself, it may be related to OA as the disease affects the whole joint. (Figure 5, [E]). More edemas can be seen in the MTP as well. (Figure 5, ([F])

Lastly there is a presence of osteophytes on many areas of the bones making up the knee joint, including the patella, MFC, trochlea, LTP, and MTP (Figure 6, [A], [C]-[F].

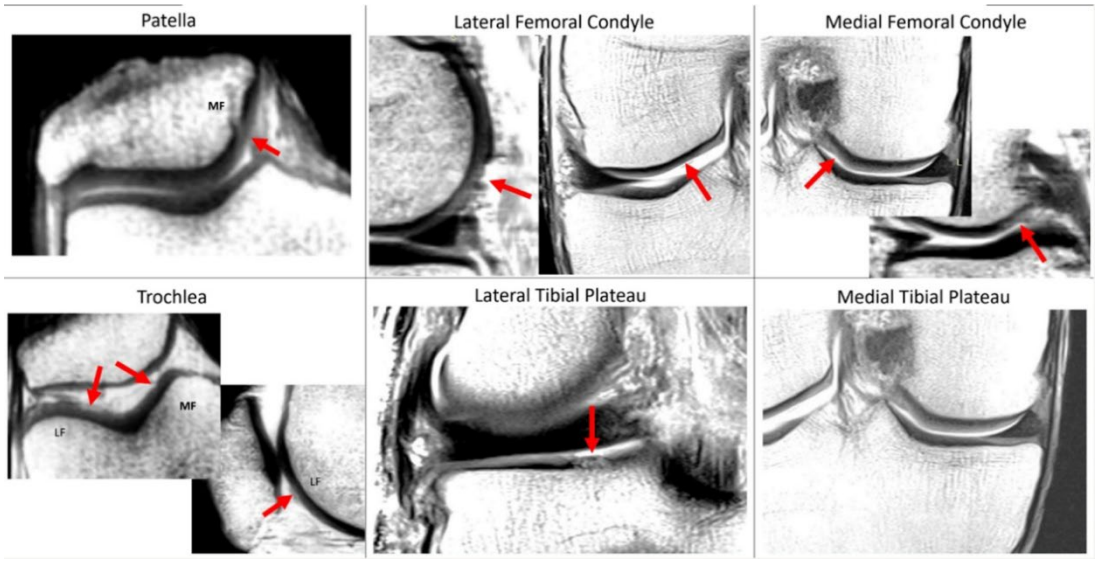

Figure 4: Cartilage changes in the right knee of subject 1.

Image [A] shows cartilage loss lining the deep aspect of the patella in the axial plane. [B] shows cartilage loss of the lateral femoral condyle in two sequencing methods. [C] the medial femoral condyle shows evidence of cartilage degradation in the coronal plane of two sequences. [D] presents axial images using two sequences, pointing out blurry MR signaling of the cartilage surrounding the trochlea. [E] shows cartilage degradation on the lateral tibial plateau. [F] presents no signs of cartilage loss around the medial tibial plateau.

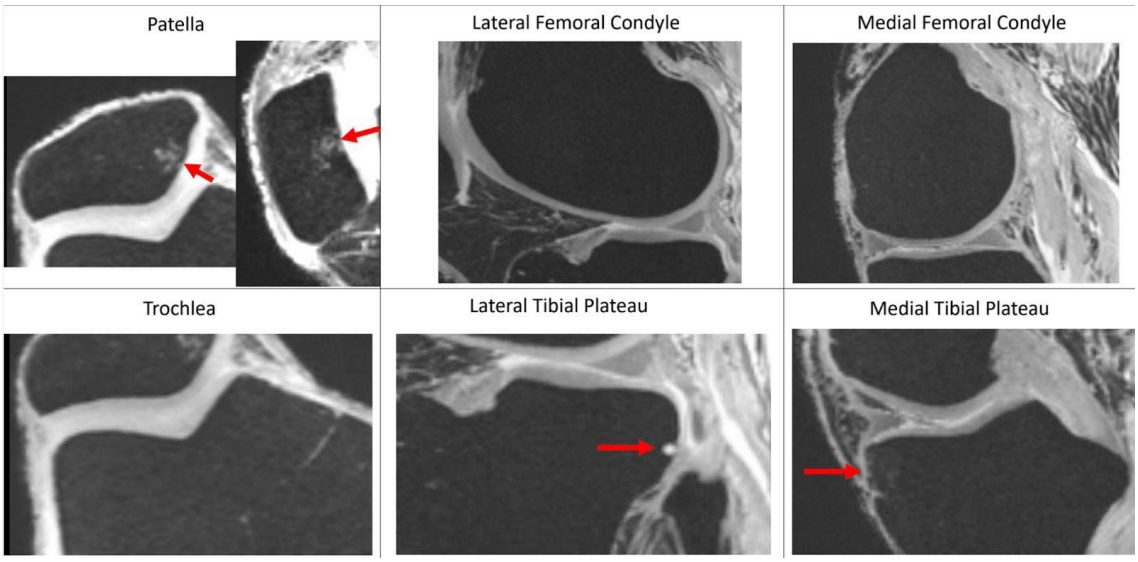

Figure 5: Bone marrow edema (BME) and cysts within the right knee of Subject 1.

Image [A] shows potential edema within the patella in the axial plane. [E] shows a minor cyst within the lateral tibial plateau in the sagittal plane that does not lie on the cartilage itself. [F] identifies more edema in the sagittal plane, located in the medial tibial plateau. [B]-[D]] show no evidence of edema or cysts in the condyles or trochlea of the right knee.

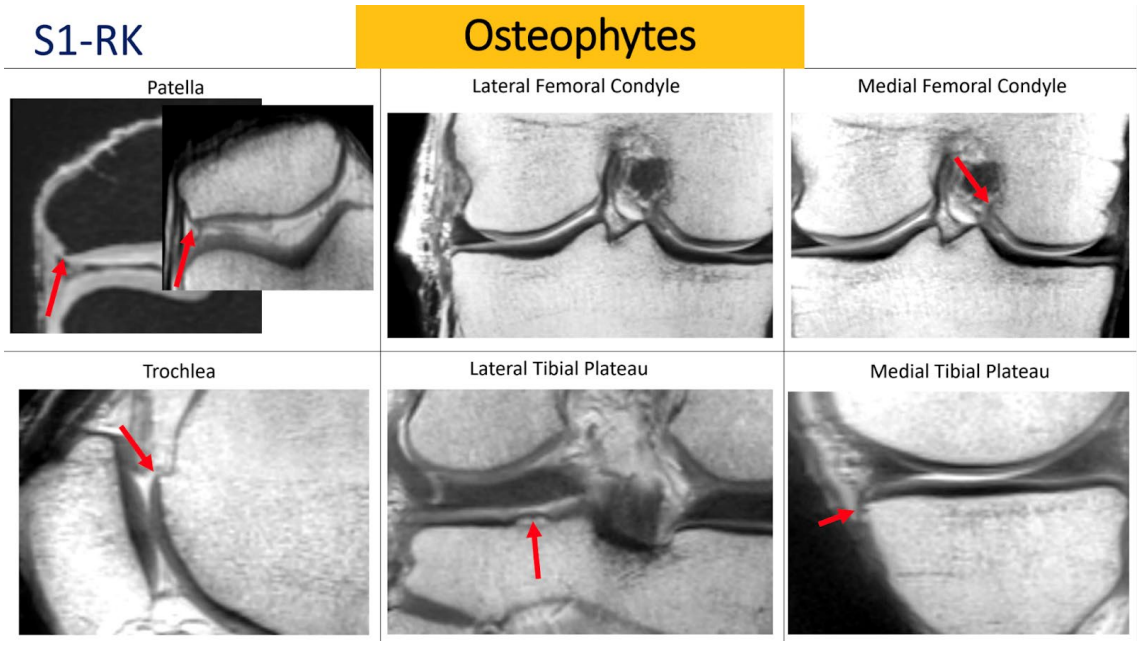

Figure 6: Presence of osteophytes in Subject 1 right knee.

Image [A] suggests that the patella has a pointed spur on its deep medial edge, displaying an osteophyte evident in several sequences. [C] points out an osteophyte in the medial femoral condyle. [D] shows a pointed spur on the trochlea as the trochlea is not lined smoothly. [E] shows a flatter, wider spit on the lateral tibial plateau. [F] shows a very minor osteophyte on the medial tibial plateau. This cartilage documentation is based on the PD/T2 scans.

Signs of lesions or extrusions in the menisci and ligaments are also present in Subject 1's right knee (Figure 7, [A]-[F]). These appear as discolorations in the images suggesting injury, tear, or extrusion to the structures. While the ligaments appear to be relatively healthy and intact, there is presence of bursae and some wearing down of the ligaments (Figure 8).

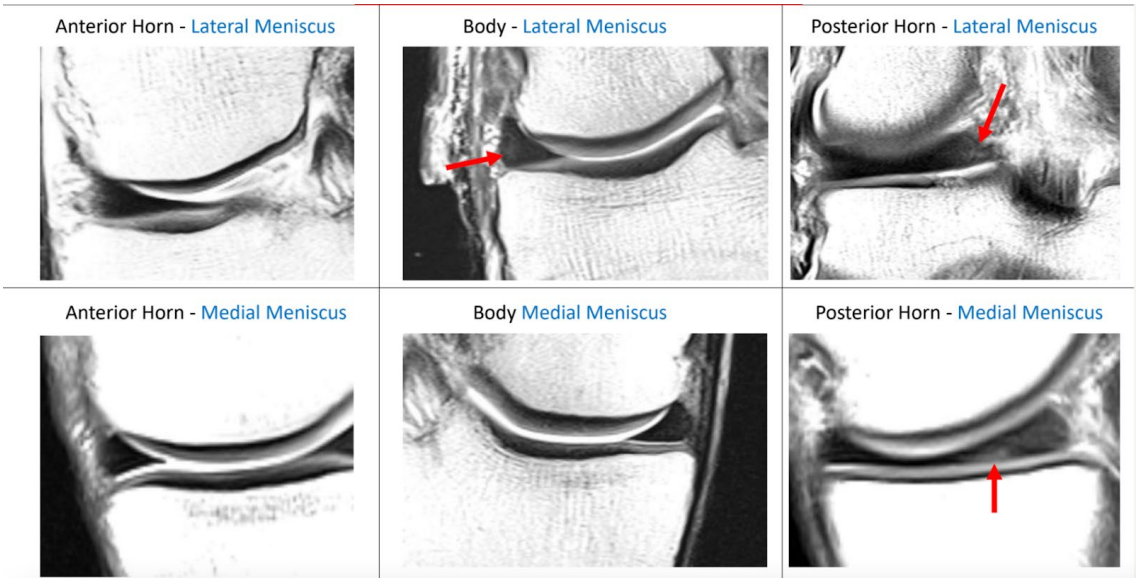

Figure 7: Meniscus lesion and extrusion in the right knee of Subject 1

Image [B] shows a slight discoloration in the body of the lateral meniscus, pointing towards a lesion in the coronal plane. [C] shows a similar sign to [B] in the posterior horn of the lateral meniscus. [F] shows a brighter appearance in the low-contrast meniscus suggesting a lesion in the posterior horn of the medial meniscus.

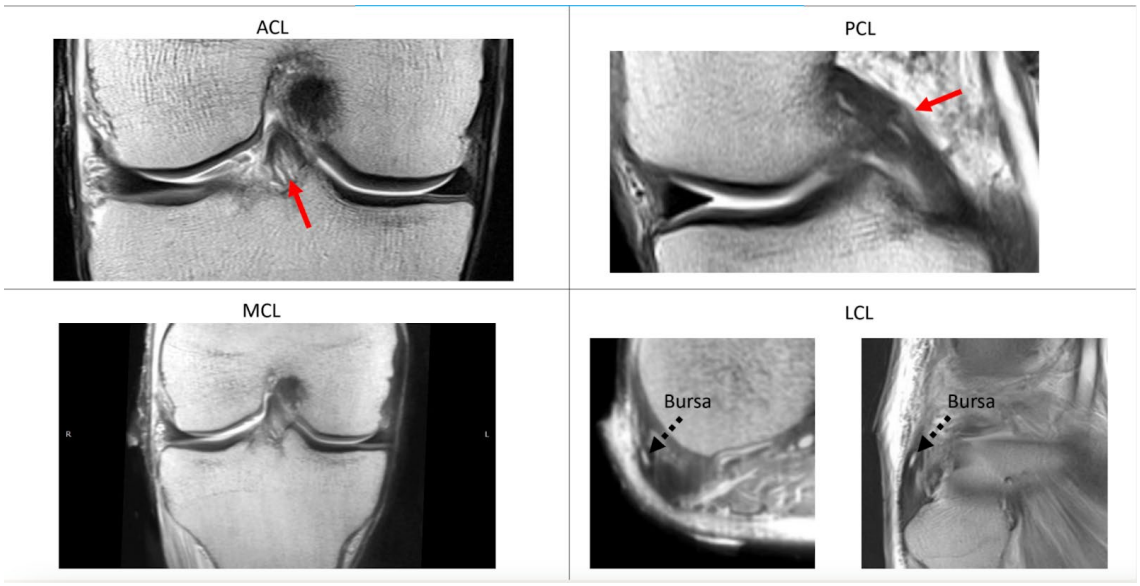

Figure 8: Ligament extrusions in the right knee of Subject 1

[A], [B] both show potential wearing down of both the anterior and posterior collateral ligaments (ACL, PCL). [D] shows the presence of bursae in both images of the lateral collateral ligament (LCL). Ligaments appear to be healthy despite the fluid between the bundles of LCL (bursae).

Inflammation within the synovial fluid is another key pathological feature of OA. Subject 1's right knee shows 3 total signs of synovitis (Figure 9). Brighter signaling within the fat pads is evident of these signs.

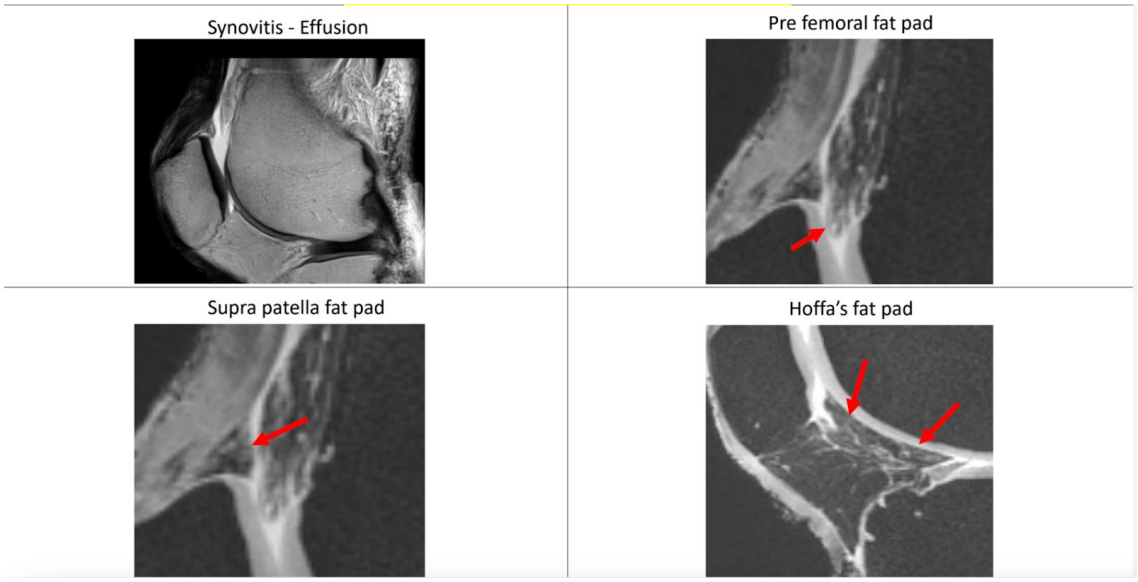

Figure 9: Signs of Synovitis in Subject 1's right knee.

[B-D] all show signs of fluid accumulation and synovitis within three of the four pat pads of the knee: pre femoral fat pad, supra patella fat pad, and Hoffa's fat pad.

Based on the amount and severity of cartilage degradation, presence of osteophytes, cysts, and bursae, and extrusion in the ligaments and menisci of Subject 1's right knee, the MRI images above presented with several signs associated with OA. Using the UCSD grading scale, OA severity and extent was measured at a 27/69, suggesting that a moderate form of OA had developed within the right knee of Subject 1 (Figure 10).

SUB 1 RK									
Features		Score		Pat	Troch	LFC	LTP	MFC	MTP
Cartilage Los	Severity	0-2	none, partial, full	1	1	1	1	1	0
	Extent	0-2	none, <50%, >50%	1	2	1	1	1	0
BME or Cyst	Sev	0-2	none, mod, sev	1	0	0	1	0	1
Osteophytes	Size/Ext	0-1	absent, present	1	1	0	1	1	1
				ALM	BLM	PLM	AMM	BMM	PMM
Meniscus	Sev	0-2	norm, deg, tear	0	1	1	0	0	1
Meniscus Ext	Sev	0-1	<2mm, >2mm		0			0	
				ACL	PCL	MCL	LCL		
Ligaments	Sev	0-2	norm, deg, tear	1	1	0	0		
				Syn					
Synovitis/eff	Sev	0-1	none, mod, sev	0					
Fat pat alt Sl	N/Y	0-1		FP					
Pre fem				1					
Supra fat				1					
Hoffa				1					
TOTAL				27					

Figure 10: Breakdown of OA grade for Subject 1's right knee using UCSD grading system

The table above represents the OA grade for Subject 1's right knee based on the grade given to each category of OA pathologies. Cartilage, BME, and osteophyte presence was graded to be a total of 19 based on whether these features were evident on the patella, trochlea, LFC, LTP, MFC, and MTP, all categorized into the red box above. Meniscus extrusion and ligament structure was also graded in the blue and green boxes, totaling to a grade of 5 as non-severe grade-1 signs were seen in the bLM, pLM, pMM, ACL, and PCL. Lastly, signs of OA were evident in fat pad inflammation within the prefemoral fat pad, supra patella fat pad, and Hoffa's fat pad, presenting with individual grades of 1 for that category, shown in the gray box. Grades were added up to a total of 27, representing moderate OA in the right knee.

Dissection Results: Subject 1- Right Knee

Upon direct analysis of the same right knee of Subject 1 mentioned in the previous section, there were several findings of cartilage degradation and minor osteophytes (Figure 11).

Shown through red circles in the images below, the medial femoral condyle presented with a significant loss of cartilage and was noticed through the touch of a large divot or dip in what should be a smooth articular surface (Figure 11). There was

also degeneration felt in the lateral condyle, trochlea, and patella (Figures 11,12). The smaller black circles represent the tiny osteophytes seen through dissection as well (Figures 11, 12).

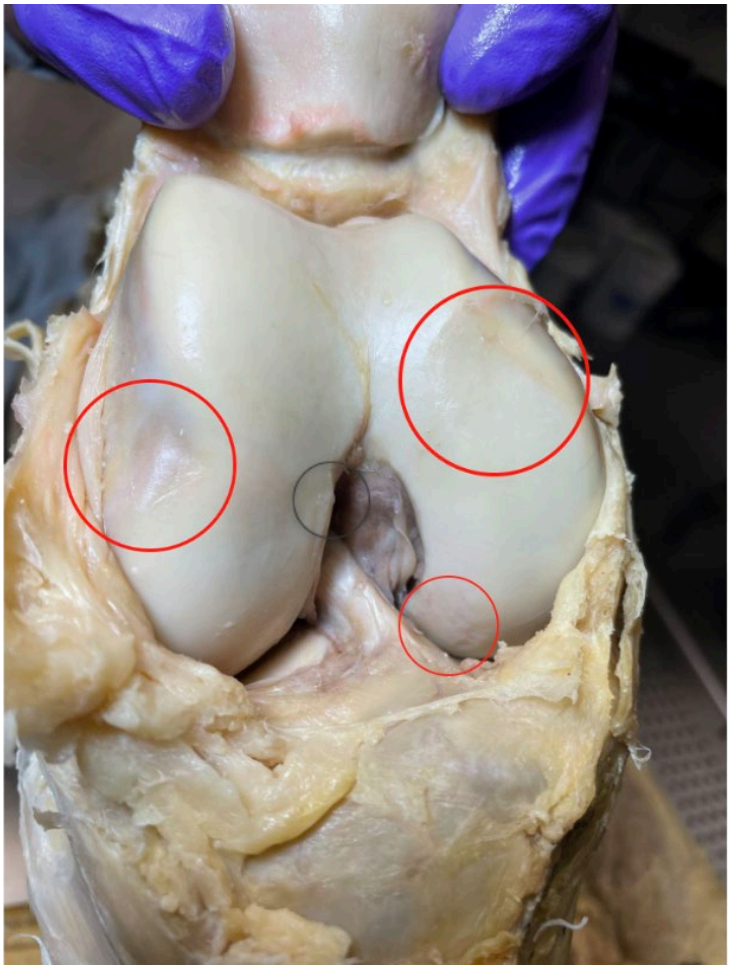

Figure 11: Anterior Dissection of Subject 1's Right Knee

The image above shows the right knee of Subject 1 in a passively flexed position following its dissection and removal of the patellar tendon. The red circles above depict the areas of cartilage loss or degeneration seen in both the lateral and femoral condyles.

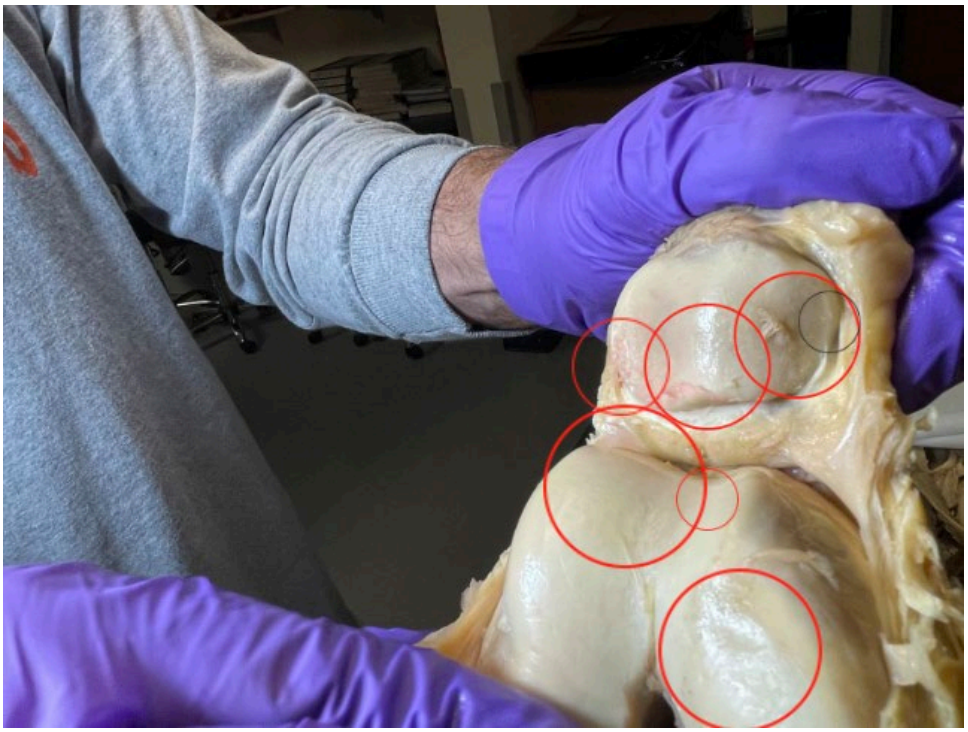

Figure 12: Trochlea and Patella of the Anterior Dissection of Subject 1's Right Knee

The image above focuses on the posterior patella and trochlea upon dissection and passive flexion. The red circles depict cartilage loss while the black circle represents the presence of an osteophyte as seen in the patella above.

Imaging Results: Subject 1- Left Knee

The left knee of Subject 1 was the next set of sequences analyzed by Dr. Chung and Dr. Mohana-Borges, again using the UCSD OA grading scale to assess the whole-joint disease and its present pathological features. The key MRI images showing evident signs of OA can be found in Appendix A, which supports the following results and grade-breakdown presented below (Figure 13). Low-grade cartilage loss was found in the LFC, trochlea, LTP, and MTP, and these minor signs are represented by divots in the articular cartilage. Two signs of BME were discovered in the patella, which showed significant fluid accumulation, and the MFC, which showed less edema. Cysts were also found in the LTP and MTP but were minor and seemingly low-grade. There were

quite a few tiny osteophytes found within multiple bony prominences, including different areas of the patella, the MFC, trochlea, and MTP. This concluded the findings for cartilaginous and bony OA features, resulting in a grade of 16 for that individual category (Figure 13).

A minor peripheral tear was found in the pMM, surrounded by degeneration and tiny meniscus cysts. There was also slight degradation seen in the bMM. The ligaments were victims to the clearest OA signs in Subject 1's left knee. The PCL was completely torn with high grade partial tears within the MCL. The ACL and LCL showed minor signs of degradation. However, due to the significance of ligament injury, the grade for the meniscus and ligament category was an 8 (Figure 13).

Lastly, joint fluid had accumulated in several spaces of the joint, and synovitis was present. Inflammation of the pre femoral fat pad, supra patella fat pad, and Hoffa's fat pad were all minimally present, resulting in a grade of 4 (Figure 13).

The left knee of Subject 2 presented with more signs of OA. Partial and complete ligament tears equate to individual grades of a 2 in that a score of 1 would only signify degeneration of the ligament in question. Cartilage loss and BME was evident, yet osteophyte presence was minimal. The overall grade of OA in Subject 1's left knee was a 28/69, signifying a minimally higher grade of moderate OA compared to Subject 1's right knee (Figure 13).

SUB 1 LK										
Features		Score		Pat	Troch	LFC	LTP	MFC	MTP
Cartilage Los	Severity	0-2	none, partial, full	0	1	0	1	0	2
	Extent	0-2	none, <50%, >50%	0	1	0	1	0	1
BME or Cyst	Sev	0-2	none, mod, sev	2	0	0	1	1	1
Osteophytes	Size/Ext	0-1	absent, present	1	1	0	0	1	1
				ALM	BLM	PLM	AMM	BMM	PMM
Meniscus	Sev	0-2	norm, deg, tear	0	0	0	0	1	1
Meniscus Ext	Sev	0-1	<2mm, >2mm		0			1	
				ACL	PCL	MCL	LCL		
Ligaments	Sev	0-2	norm, deg, tear	1	2	1	1		
				Syn					
Synovitis/eff	Sev	0-1	none, mod, sev	1					
Fat pat alt Sl	N/Y	0-1		FP					
Pre fem				1					
Supra fat				1					
Hoffa				1					
TOTAL				28					

Figure 13: Breakdown of OA grade for Subject 1's left knee using UCSD grading system.

Highlighted in the red box, cartilage loss and bony features of OA were present in all cartilaginous and bony areas of the knee. Cartilage loss was present in the trochlea, LTP, and MTP, where severity was highest at a grade 2. BME was severe in the patella at a grade of 2, but also present in the MFC, while cysts were found LTP and MTP. Tiny osteophytes were found in the patella, trochlea, MFC, and MTP, resulting in individual grades of 1 signifying their presence. Meniscus degradation was only found in the bMM and pMM with grades of 1 due to minimal tearing. Ligament tearing was found at low grades in the ACL, MCL, and LCL; however, PCL presented with a complete tear at grade 2. Lastly, synovitis and inflammation was minimally evident in the synovium, pre femoral fat pad, supra patella fat pad, and Hoffa's fat pad. The total grade was calculated to be a 28, signifying a more severe form of moderate OA compared to Subject 1's right knee.

Dissection Results: Subject 1-Left Knee

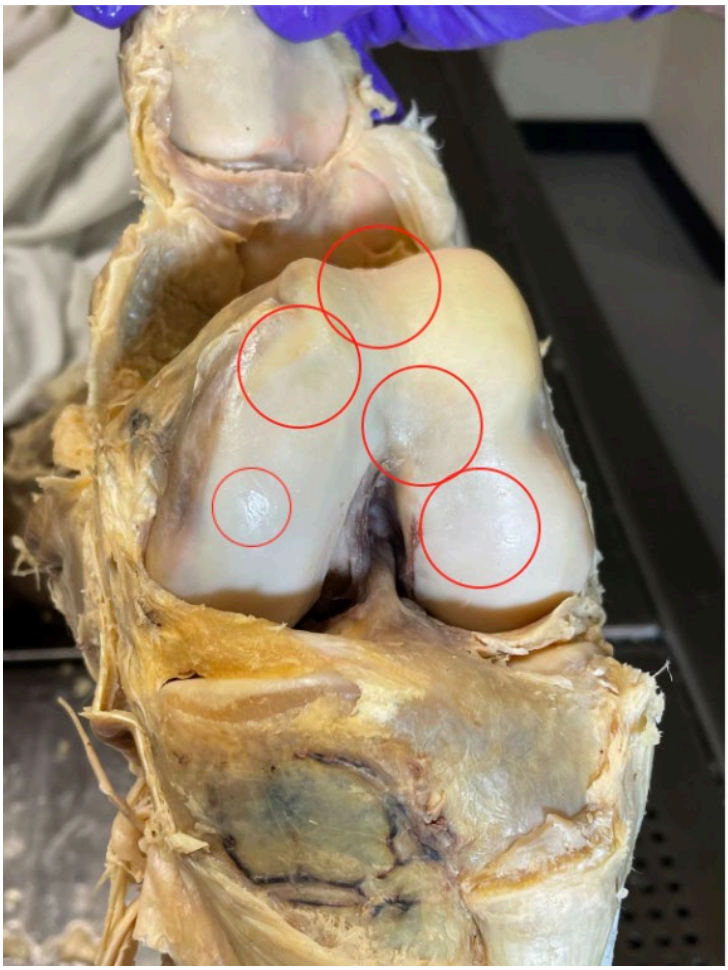

Figure 14: Anterior Dissection of Subject 1's Left Knee

The image above shows the left knee of Subject 1 in a passively flexed position following its dissection and removal of the patellar tendon. The red circles above depict the areas of cartilage loss or degeneration seen in the trochlea and lateral and femoral condyles.

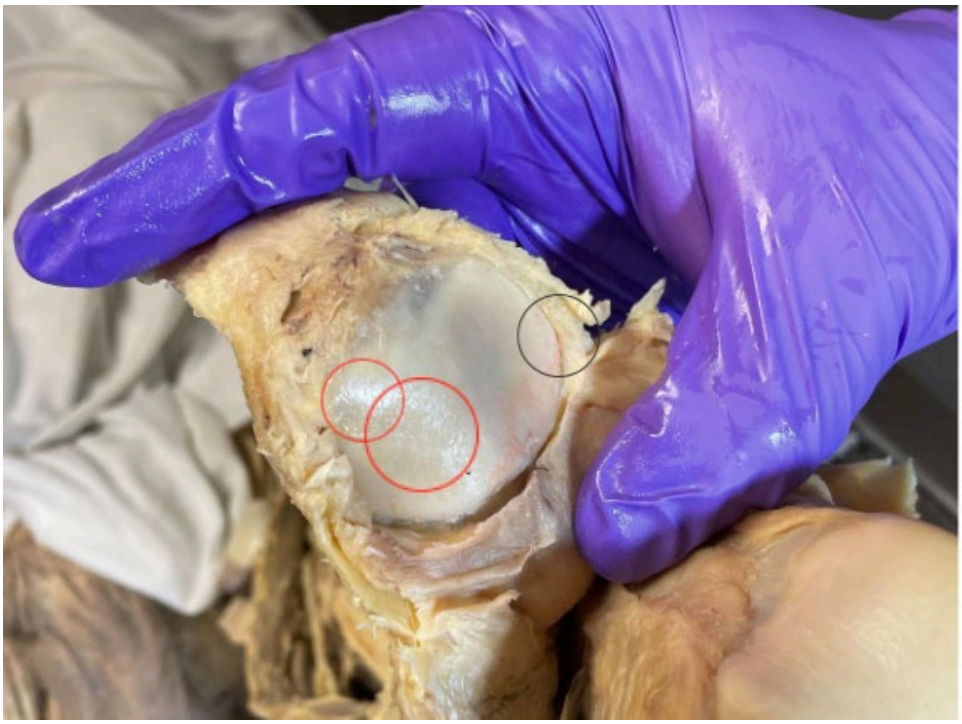

Figure 15: Patella of the Anterior Dissection of Subject 1's Left Knee

The image above focuses on the posterior patella upon dissection and passive flexion of the knee. The red circles depict cartilage loss while the black circle represents the presence of an osteophyte as seen in the patella above.

Imaging Results: Subject 2-Right Knee

Appendix B provides MRI images of key OA findings for Subject 2's right knee, with evidence as follows. Cartilage loss was seen around the patella, LF, and MFC, while the other three structures appeared to maintain a healthy coating of cartilage. Minor cysts were also noted in the LFC, LTP, and MTP, while BME was absent. Lastly in this category, the patella, LFC, MFC, and MTP each presented with small osteophytes.

The menisci of Subject 2's right knee appeared relatively healthy through MRI imaging, with minimal degradation seen in the bLM and pLM. Ligaments also

presented with minimal OA pathological features, as the ACL and PCL only showed signs of slight wearing.

Fluid accumulation within the pre femoral fat pad, supra patella fat pad, and Hoffa's fat pad was spotted; however, synovitis was absent.

With no cartilage loss on either tibial plateau, minimal fat pad swelling and osteophyte presence, and no evidence suggesting meniscus/ligament tearing, the right knee of Subject 2 showed lesser signs of OA compared to either knee of Subject 1. The total grade of OA was concluded to be a 20/69, displaying low-grade mild OA. (Figure 16).

SUB 2 RK									
Features		Score		Pat	Troch	LFC	LTP	MFC	MTP
Cartilage Los	Severity	0-2	none, partial, full	1	0	1	0	1	0
	Extent	0-2	none, <50%, >50%	1	0	1	0	1	0
BME or Cyst	Sev	0-2	none, mod, sev	0	0	1	1	0	1
Osteophytes	Size/Ext	0-1	absent, present	1	0	1	0	1	1
				ALM	BLM	PLM	AMM	BMM	PMM
Meniscus	Sev	0-2	norm, deg, tear	0	1	1	0	0	0
Meniscus Ext	Sev	0-1	<2mm, >2mm		0			0	
				ACL	PCL	MCL	LCL		
Ligaments	Sev	0-2	norm, deg, tear	1	1	0	0		
				Syn					
Synovitis/eff	Sev	0-1	none, mod, sev	0					
Fat pat alt Sl	N/Y	0-1		FP					
Pre fem				1					
Supra fat				1					
Hoffa				1					
TOTAL				20					

Figure 16: Breakdown of OA grade for Subject 2's right knee using UCSD grading system.

Cartilage loss, highlighted in the first two red rows of the figure, was moderately severe with minimal extent supported by the grades of 1 within the patella, LFC, and MFC. The third red row signifies the three grade-1 cysts within the LFC, LTP, and MTP. Lastly, within the cartilage and bone section, osteophytes were present in the patella, LFC, MFC, and MTP, resulting in individual grades of 1. The blue section, representing meniscus tearing, shows grades of 1 in the bLM and pLM due to minor wearing. Minor ligament degradation is shown in the green section, displaying low grades of 1 in the ACL and PCL. Lastly, synovitis appears to be absent in the yellow box while the gray box highlights the presence of inflammation within the pre femoral fat pad, the supra patella fat pad, and Hoffa's fat pad, with grades of 1 symbolizing their presence. The final OA grade was added up to be a 20/69, representing mild OA in the right knee of Subject 2.

Dissection Results: Subject 2-Right Knee

Cartilage degradation was seen in both femoral condyles, the trochlea, and the patella (Figures 17, 18). A minor osteophyte was also felt in the trochlea and patella (Figures 17, 18).

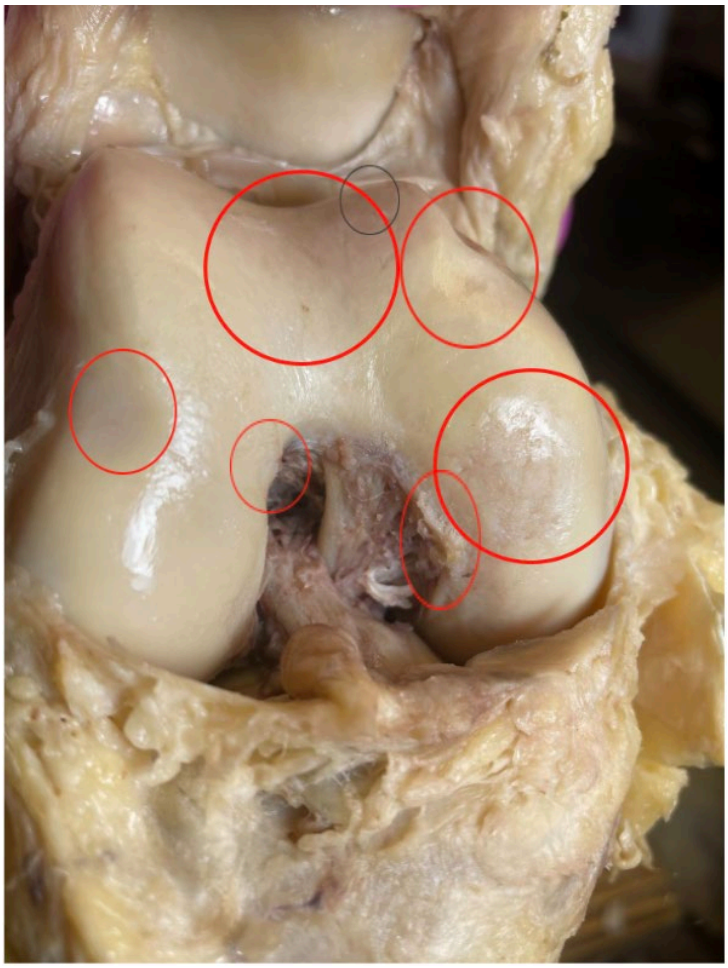

Figure 17: Anterior Dissection of Subject 2's Right Knee

The image above shows the right knee of Subject 2 in a passively flexed position following its dissection and removal of the patellar tendon. The red circles above depict the areas of cartilage loss, as seen in the femoral condyles and trochlea. A minor osteophyte was also seen in the trochlea.

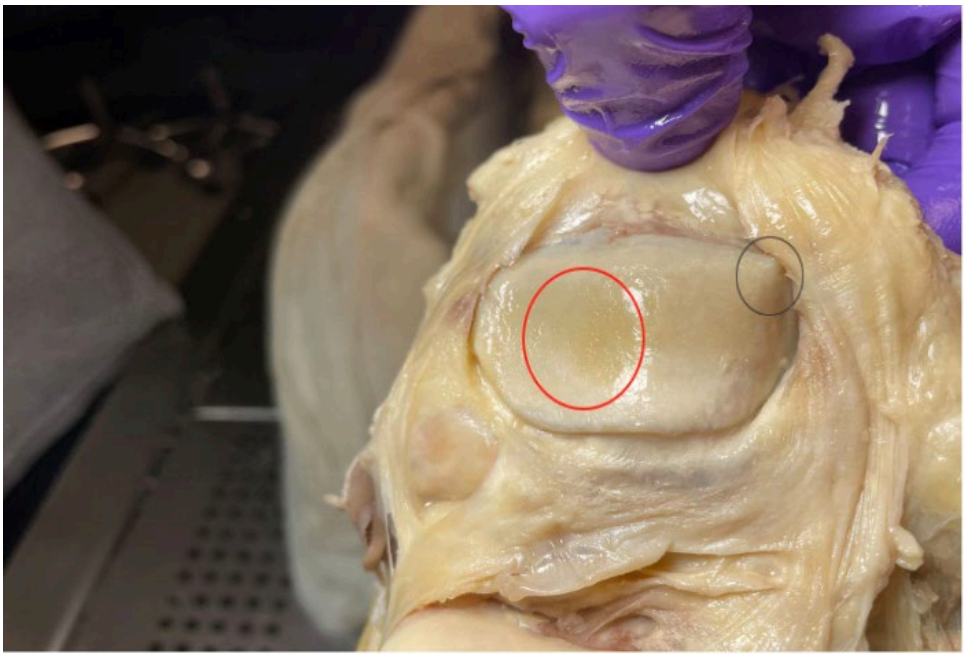

Figure 18: Patella of the Anterior Dissection of Subject 2's Right Knee

The image above focuses on the posterior patella upon dissection and passive flexion of the knee. The red circles depict cartilage loss while the black circle represents the presence of an osteophyte as seen in the patella above.

Imaging Results: Subject 2-Left Knee

The last knee analyzed by Dr. Chung and Dr. Mohana-Borges was the left knee of Subject 2. Grading steps were repeated for this knee following the analysis of key images with OA findings, found in Appendix C. Cartilage loss was only present in the LFC and MFC shown by the minor changes in signal in the lining of cartilage. Only one minor cyst was discovered in the MTP, while BME was completely absent in all structures. Osteophytes were present on the bony structures of the patella, LFC, MFC, LTP, and MTP.

No OA-related changes were found within the menisci of the knee. Slight wearing, however, was discovered in the ACL, PCL, and MCL, with a small bursa present in the MCL.

Lastly, inflammation was seen in both the pre femoral fat pad and supra patella fat pad. Despite no evidence of effusion, there was synovitis detected in the suprapatellar patch.

Subject 2's left knee resulted with the least number of signs of OA based on the minimal evidence found using the UCSD grading scale. Minor degradation in the cartilage, bones, and ligaments was found, and no signs of meniscus effusion was evident. However, there remained signs of cartilage loss, ligament wearing, BME, and osteophytes, which suggested that some level of OA was still present. A grade of 17 was assigned to Subject 2's left knee, and despite its superior health over the other three knees, still classifies as a mild grade of OA.

SUB 2 LK									
Features		Score		Pat	Troch	LFC	LTP	MFC	MTP
Cartilage Los	Severity	0-2	none, partial, full	0	0	1	0	1	0
	Extent	0-2	none, <50%, >50%	0	0	1	0	2	0
BME or Cyst	Sev	0-2	none, mod, sev	0	0	0	0	0	1
Osteophytes	Size/Ext	0-1	absent, present	1	0	1	1	1	1
				ALM	BLM	PLM	AMM	BMM	PMM
Meniscus	Sev	0-2	norm, deg, tear	0	0	0	0	0	0
Meniscus Ext	Sev	0-1	<2mm, >2mm		0			0	
				ACL	PCL	MCL	LCL		
Ligaments	Sev	0-2	norm, deg, tear	1	1	1	0		
				Syn					
Synovitis/eff	Sev	0-1	none, mod, sev	1					
Fat pat alt Sl	N/Y	0-1		FP					
Pre fem				1					
Supra fat				1					
Hoffa				0					
TOTAL				17					

Figure 19: Breakdown of OA grade for Subject 2's left knee using UCSD grading system.

Cartilage loss, highlighted in the first two red rows of the figure, was only present in the LFC and MFC where severity was at a grade 1 but extent was a grade 2 for the MFC due to the amount of loss evident. One minor cyst was found in the MTP, shown in the third row of the red box. The last OA feature within the bone and cartilage was osteophyte presence, seen in the last row of the red box, where these features were found in the patella, LFC, MFC, LTP, and MTP, resulting in individual grades of 1. The blue section represents the OA signs within the menisci, which were absent in Subject 2's left knee. Ligament degradation is shown in the green section, displaying low grades of 1 in the ACL, PCL, and MCL. Lastly, synovitis was discovered, as seen in the yellow box, while the gray box highlights the presence of inflammation within the pre femoral fat pad and supra patella fat pad with grades of 1 simply symbolizing their presence. The OA grade was determined to be a 17/69, representing the lowest grade of mild OA between all four knees in this experiment.

Dissection Results: Subject 2 – Left Knee

Due to unavoidable circumstances, dissection was incomplete for the left knee of Subject 2, eliminating it from further analysis and discussion in this project.

DISCUSSION (COMPARISON)

Overview

Results from MRI were gathered by radiologists Dr. Chung and Dr. Aurea Borges who summarized and graded their findings using the UCSD grading scale mentioned in the "methods" section of this research. Interpretation of their results relied on a small scale of 0-2 or 0-1 while dissection findings fell under the same scale in a modified version of the UCSD grading scale. More detail on this form of analysis is mentioned in the "limitation" section, however it is important to note the scale used for the following tables and comparisons.

Analysis Comparison: Subject 1- Right Knee

Referring to the MRI grades (Figure 10) and the dissection findings (Figures 11, 12) for the right knee of Subject 1, comparisons can be made between the two methods of visualizations to further analyze the effectiveness of MRI diagnosis. Comparison charts were made for the two OA signs that could be compared with MRI and dissection (cartilage loss and bone abnormalities) to summarize findings and simplify comparison (Tables 1, 2, 3).

MRI did a generally good job at identifying the signs of cartilage loss that were evident in the cartilage following dissection; however, severity of cartilage loss in the medial femoral condyle was graded higher upon direct visualization due to the depth of degradation in the specific area (Table 1). MRI was not sensitive to severity in this case.

	MRI	Dissection
MFC	1	2
LFC	1	1
Patella	1	1
Trochlea	0	0

Table 1: Signs of Cartilage Loss in MRI Versus Dissection for Sub 1 Right Knee

The table above highlights the findings from both MRI and dissection, specifically regarding cartilage degradation. MRI and dissection both picked up signs of cartilage loss in both femoral condyles as well as the patella. The severity of cartilage degeneration was deemed higher in the medial femoral condyle following dissection than MRI due to the feeling of a deep lesion in the cartilage.

Analysis Comparison: Subject 1- Left Knee

The left knee of Subject 1 had more of a disparity in results when comparing MRI to dissection in analyzing cartilage integrity, as summarized by the table below (Table 2).

MRI only picked up a sign of degradation in the trochlea (and tibial plateaus which could not be analyzed through dissection). Following dissection, degradation was found in both femoral condyles as well as the patella and trochlea, showing that MRI did not pick up the minor signs that were visualized directly.

	MRI	Dissection
MFC	0	1
LFC	0	1
Patella	0	1
Trochlea	1	1

Table 2: Signs of Cartilage Loss in MRI Versus Dissection for Sub 1 Left Knee

The table above highlights the findings from both MRI and dissection, specifically regarding cartilage degradation. MRI only picked up degradation in the trochlea while cartilage loss was directly found in all areas in this specific knee.

Analysis Comparison: Subject 2- Right Knee

Cartilage loss was identified by MRI in both condyles as well as the patella. The dissection findings supported such results; however, direct visualization also presented degradation in trochlea. MRI, again, identified almost all signs of degradation found directly in the knee, besides the trochlea.

	MRI	Dissection
MFC	1	1
LFC	1	1
Patella	1	1
Trochlea	0	1

Table 3: Signs of Cartilage Loss in MRI Versus Dissection for Sub 2 Right Knee

The table above highlights the findings from both MRI and dissection, specifically regarding cartilage degradation. MRI picked up almost all signs of cartilage loss supported by dissection analysis, except for degradation found in the trochlea.

In summarizing the results found for osteophyte presence, it was evident that MRI properly identified the bone abnormalities seen through direct dissection analysis for all three knees. MRI, in fact, picked up evidence of osteophytes in areas that were not seen in dissection. This could indicate that MRI is effective in identifying such features, as such bony spurs may have been to minor to feel upon dissection.

Based on the comparative charts and findings from both indirect and direct visualization of the joint, analysis following direct dissection led to the discovery of more OA signs than MRI picked up. This suggests that MRI did not show minor pathological signs that could only be seen in the direct joint, as well as the extent of the pathology in some of the cases.

Diagnostic tools should not only be evaluated on their effectiveness in identifying cases of OA, but in assessing the severity of individual cases.

LIMITATIONS

This research was independent of any formal lab programs and therefore was accompanied by many logistical obstacles and limitations.

First, the subject pool consisted of cadaveric specimens, impacting the practicality of the study in diagnosing living people. Future studies should explore more reliable methods of OA diagnosis in comparison to MRI, as intricate dissection cannot be carried out on living humans.

Next, the study design used two of twelve donors available at the anatomy lab, and the selection was randomized to allow other anatomy students the opportunity to study the remaining donors. This small sample size only allowed for four knees to be analyzed, limiting results to few subjects. This was further limited by the delay in dissection by one of the recruited anatomy students on one of the knees, making it unavailable for direct examination. As mentioned above, the subjects' information regarding medical history was not divulged in order to ensure their privacy as donors. This eliminated any control by utilizing subjects who were at high risk of having OA, which could have been seen through their histories of activity, surgery, diagnoses, and medical conditions. While OA is not an inevitable age-related joint disease, and it can develop into both minimally and grossly defined disease, knowledge of lifestyle factors and medical histories would have allowed for the study of clearly diseased individuals.

Next, without years of professional training and due to the minimally available research on cadaveric subjects in this context, four MRI sequences commonly used for living humans suffering from OA had to be used, neglecting the possibility that different sequences might prove more efficient for examining the joint post-mortem.

Variables such as joint fluidity, stiffness, bone density, etcetera, all undergo natural changes upon death, impacting the results through imaging variability and direct assessment.

Radiologist interpretation, often seen through a formal report, is crucial in allowing physicians the proper evidence for which a specific treatment or prevention plan is initiated. In a clinical setting in which a patient is being diagnosed with OA, images are offered along with interpretation as images alone will not provide any insight to the patient on what they are observing. As there is no standard scale for diagnosing grade of OA, interpretation is somewhat subjective based on radiologist experience, opinion, and grading scale. Furthermore, there is apparently no current standard scale for grading OA. Connecting with numerous radiologists and using a plethora of scales would allow for more analyses to be used in this study.

Lastly, this study was completed amidst the COVID-19 pandemic, implementing obstacles throughout the research process. This limitation made lab availability, connecting with radiologists, anatomists, mentors, and development of a comprehensive research plan difficult; however, this research certainly resulted in a gain of knowledge and experience in project management.

CONCLUSION

The purpose of this study was to evaluate the effectiveness of the "gold standard" MRI in diagnosing and grading OA. Previous research has highlighted the uncertainty surrounding MRI's reliability as a diagnostic tool for the common joint disease. In an attempt to initiate a new route in which this controversy can be settled, this study used analytic comparison between indirect imaging and direct joint evaluation through dissection.

It was concluded that indirect visualization through MRI proved to accurately identify osteoarthritic signs within the joint based on direct evaluation through dissection. With that being said, the severity of the signs was not reflected through MRI as evidenced by missed minor signs of OA and by a lower MRI grade than dissection grade the case of Subject 1's Left Knee (Table 2)

MRI's lack of sensitivity to severity presents a problem in its diagnostic abilities, as a physician will likely attack the disease based on severity of signs rather than based on the mere presence of signs. Shown in the examples within this paper, the knees that presented with identical grades in a certain area appeared very different when looking at the joint directly. Thus, a larger scale should be used in congruence with either MRI or future diagnostic tools to better reflect the spectrum of severity of a knee's OA.

Further research should not only control the limitations presented in this research but should also aim to identify and discover new diagnostic tools that assess severity of the disease and its various pathological signs. This will allow physicians to properly understand a presented case to accurately diagnose OA and prepare suitable

treatment and prevention plans for the best results for that specific patient. Implementing new and effective tools may also lead to a better understanding of the disease, and therefore the development of new interventions, that may not even be contemplated at the present time. Finally, such enhanced tools and understanding may even lead to the discovery of a cure for OA.

Appendix A: Subject 1 Left Knee MRI Images

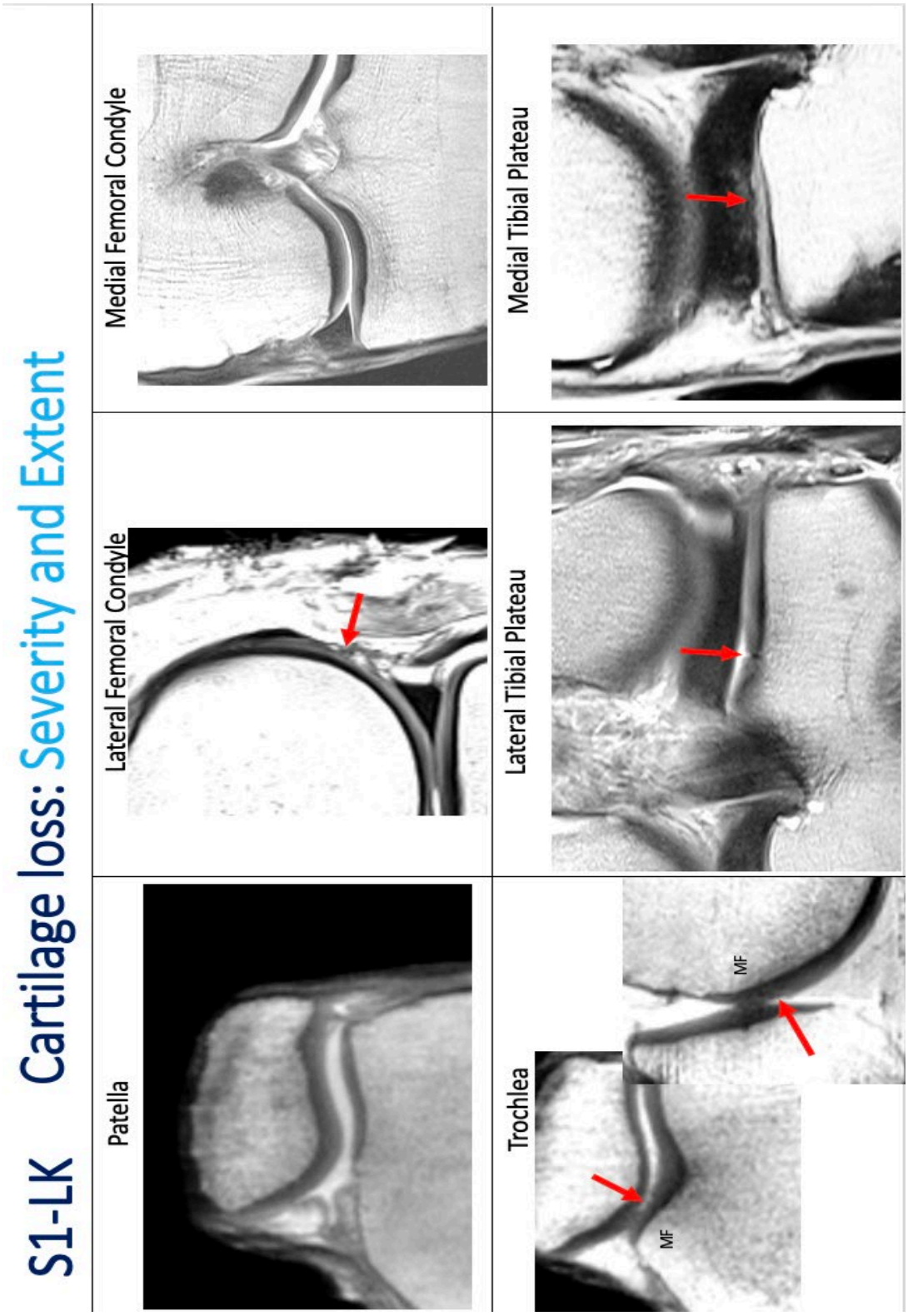

S1-LK

BME or Cyst

Patella

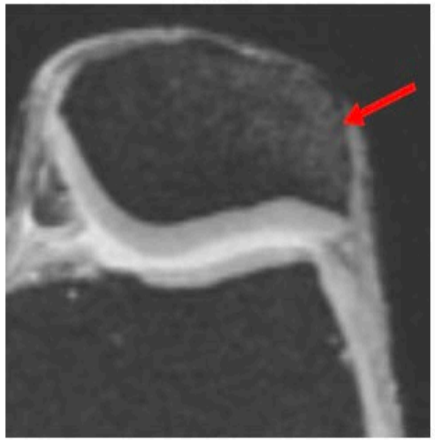

Lateral Femoral Condyle

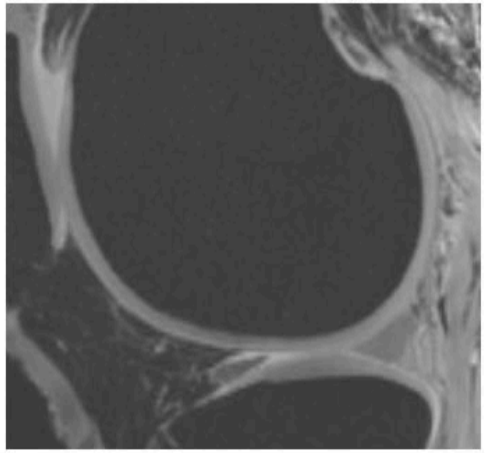

Medial Femoral Condyle

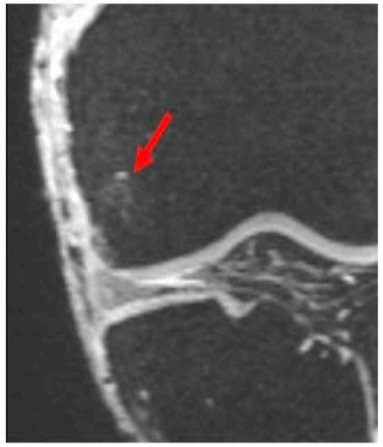

Trochlea

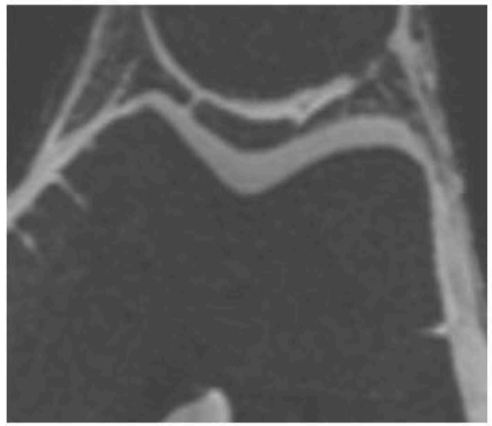

Lateral Tibial Plateau

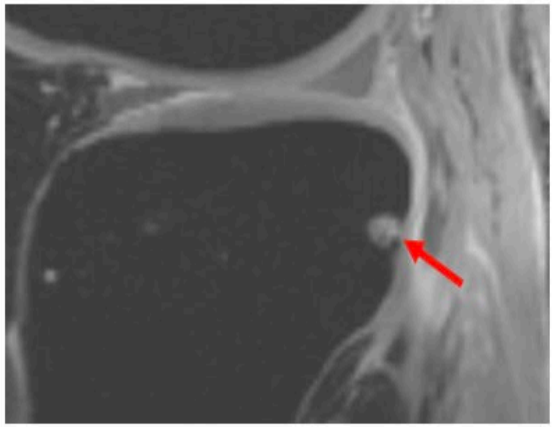

Medial Tibial Plateau

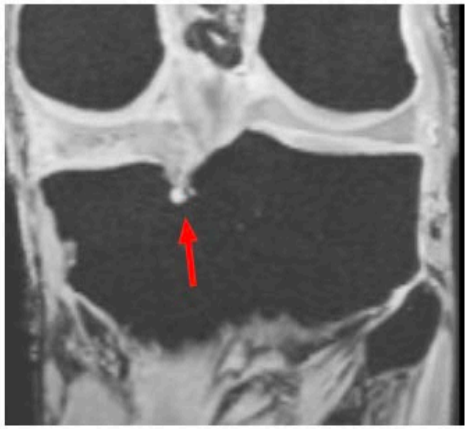

S1-LK

Osteophytes

Patella

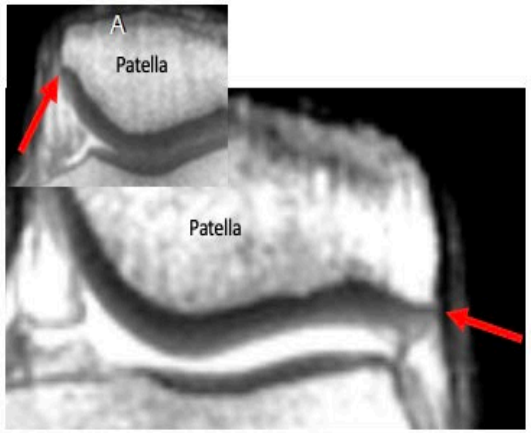

Lateral Femoral Condyle

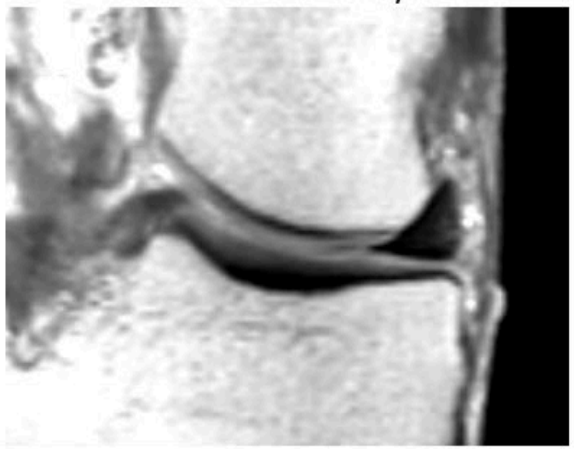

Medial Femoral Condyle

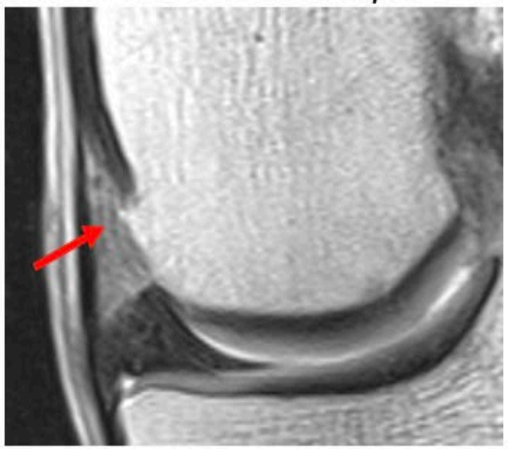

Trochlea

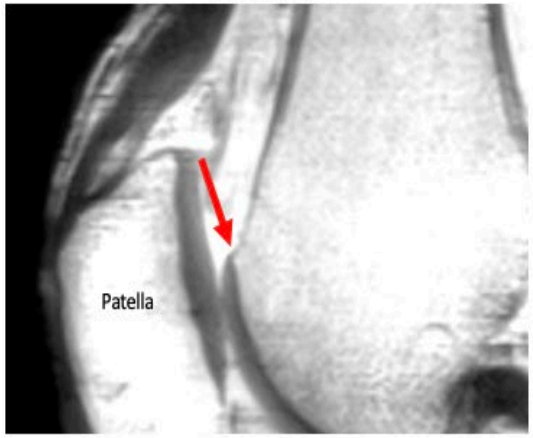

Lateral Tibial Plateau

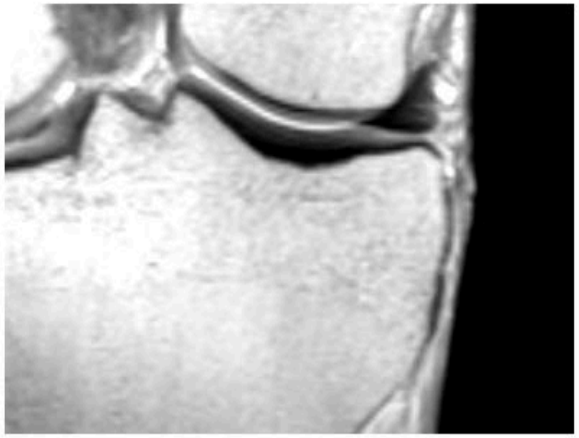

Medial Tibial Plateau

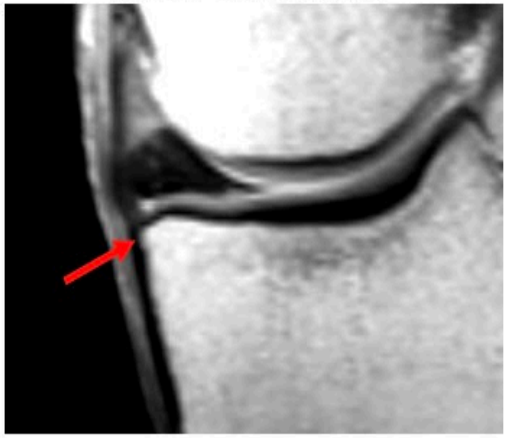

S1-LK

Meniscus: Severity

Anterior Horn - Lateral Meniscus

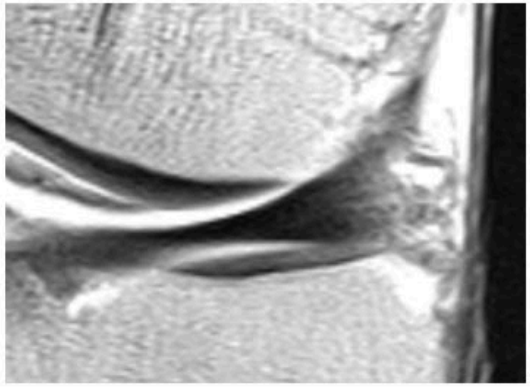

Body - Lateral Meniscus

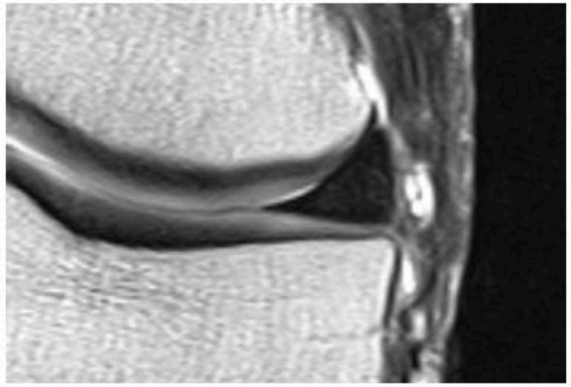

Posterior Horn - Lateral Meniscus

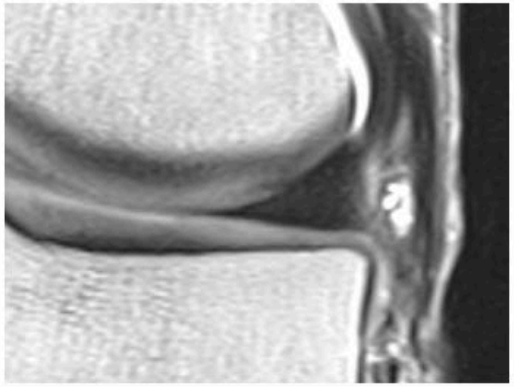

Anterior Horn - Medial Meniscus

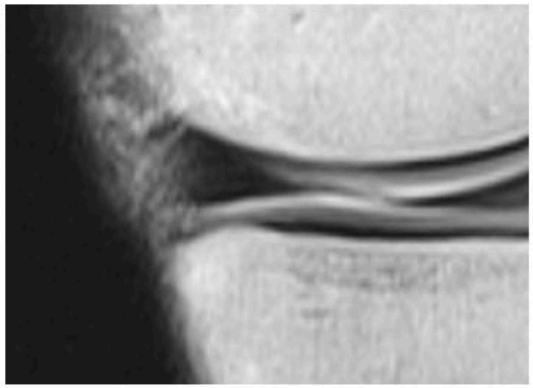

Body Medial Meniscus

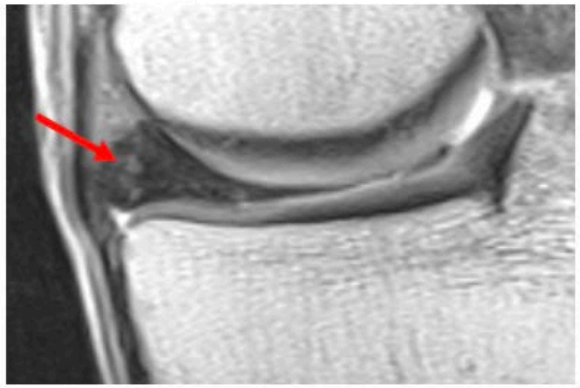

Posterior Horn - Medial Meniscus

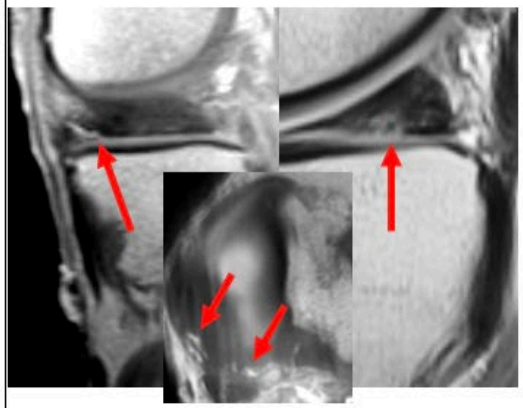

S1-LK

Ligaments

ACL

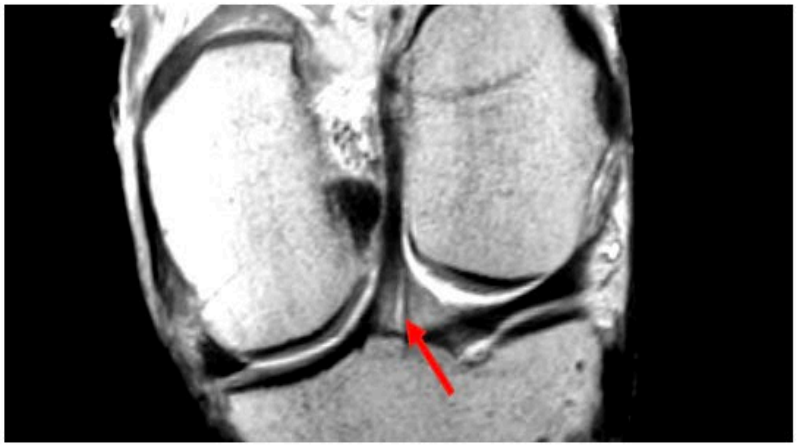

PCL

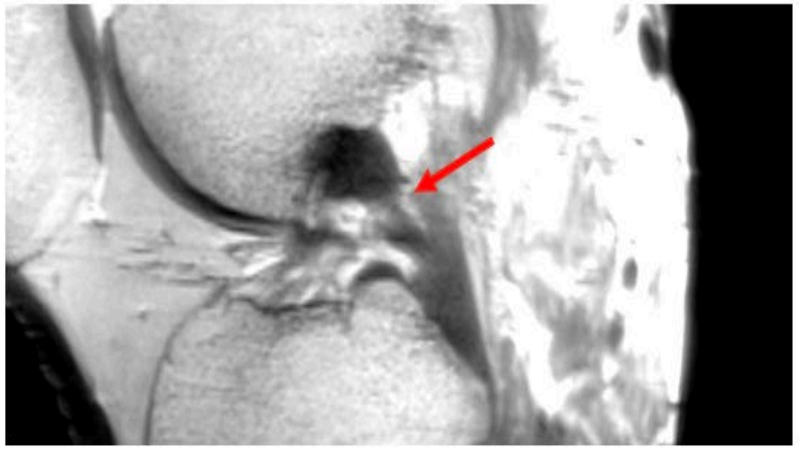

MCL

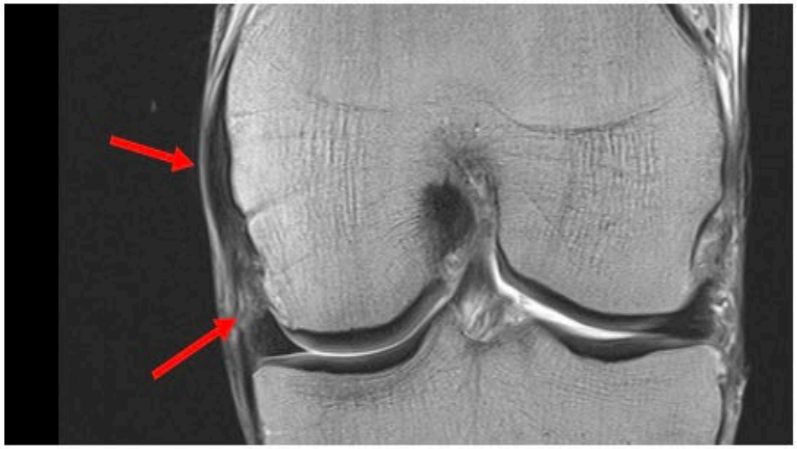

LCL

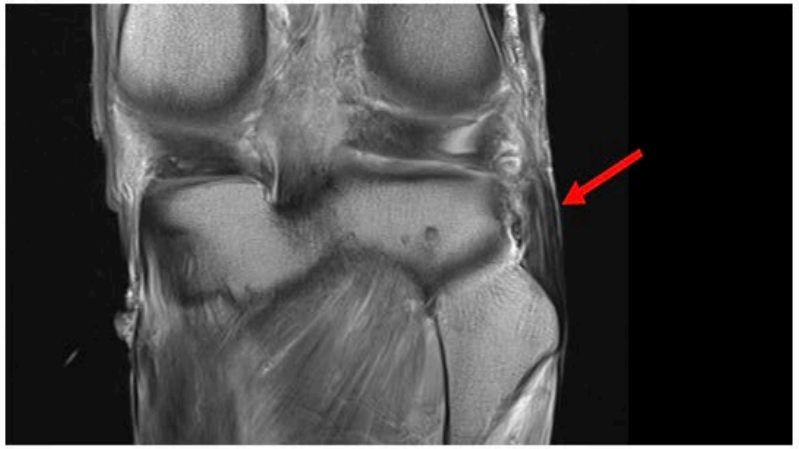

S1-LK

Synovitis / Fat Pad

Synovitis - Effusion

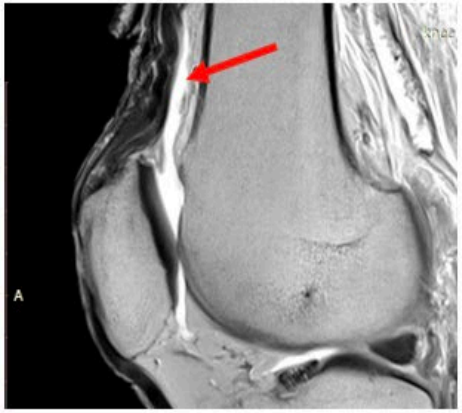

Pre femoral fat pad

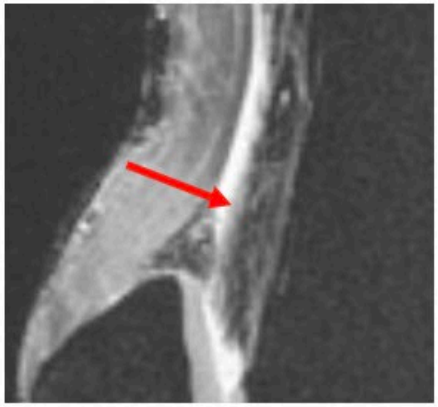

Supra patella fat pad

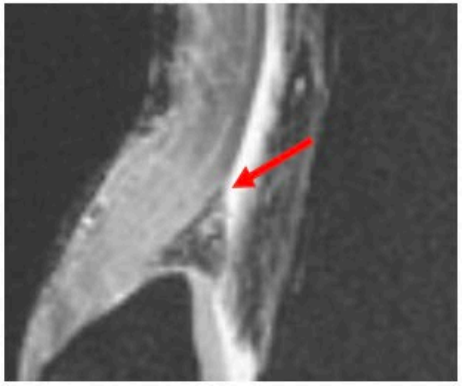

Hoffa's fat pad

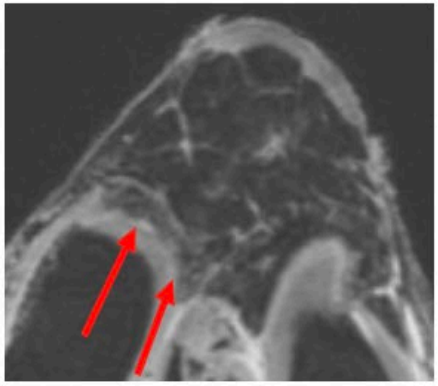

Appendix B: Subject 2 Right Knee MRI Images

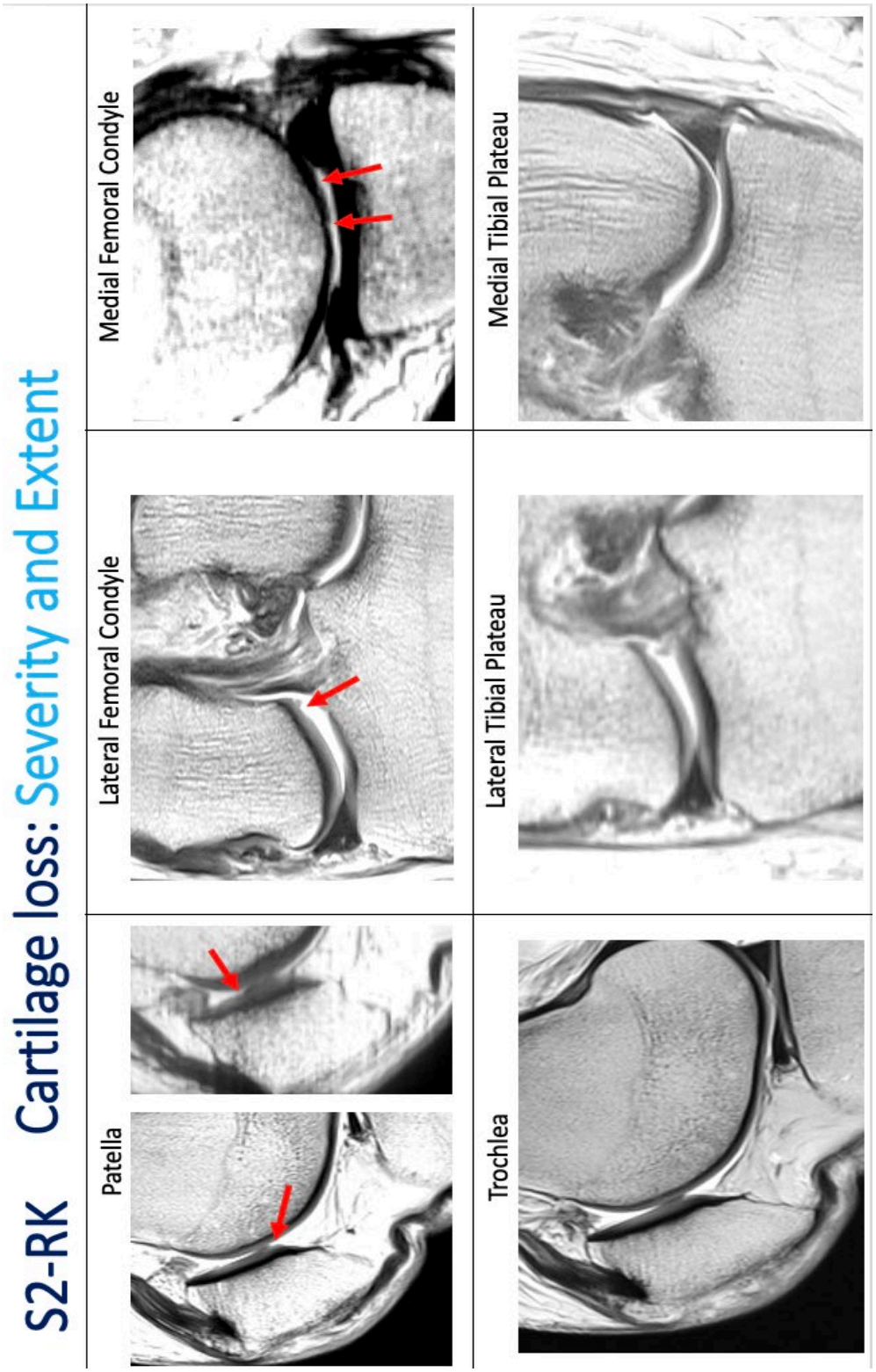

S2-RK

BME or Cyst

Patella

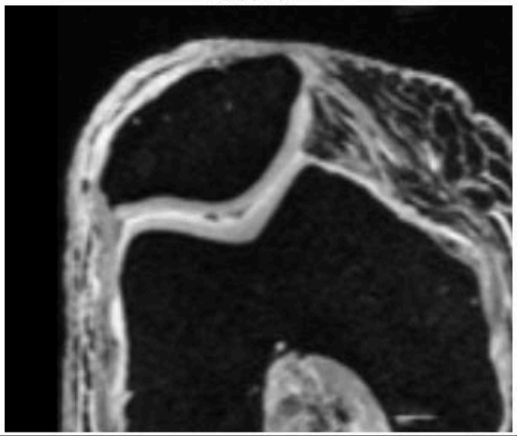

Lateral Femoral Condyle

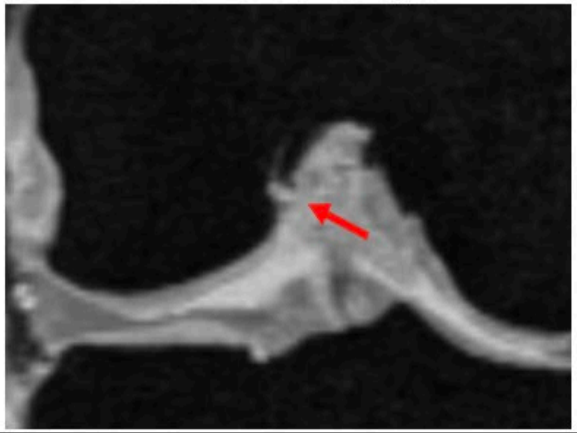

Medial Femoral Condyle

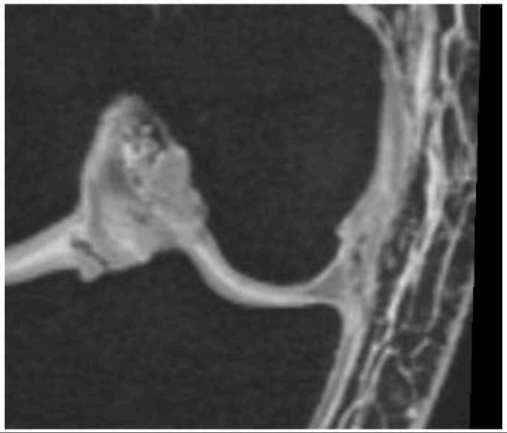

Trochlea

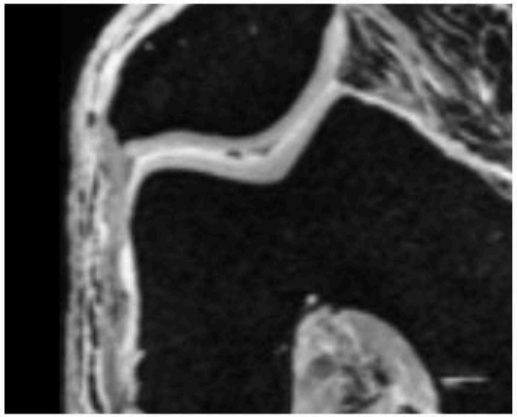

Lateral Tibial Plateau

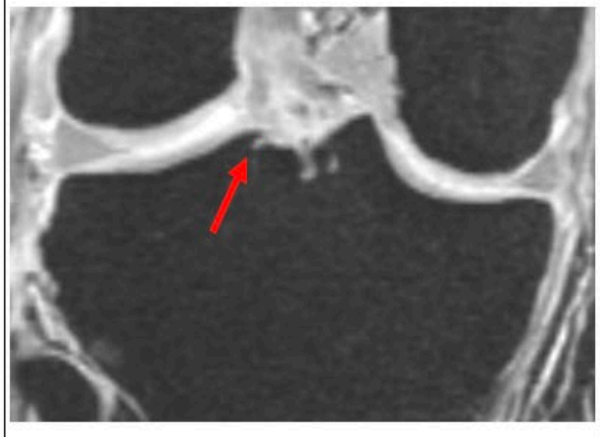

Medial Tibial Plateau

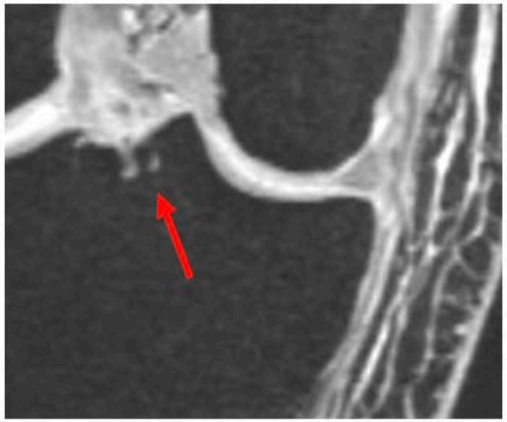

S2-RK

Osteophytes

Patella

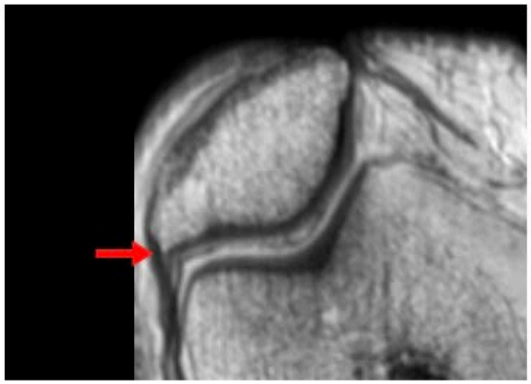

Lateral Femoral Condyle

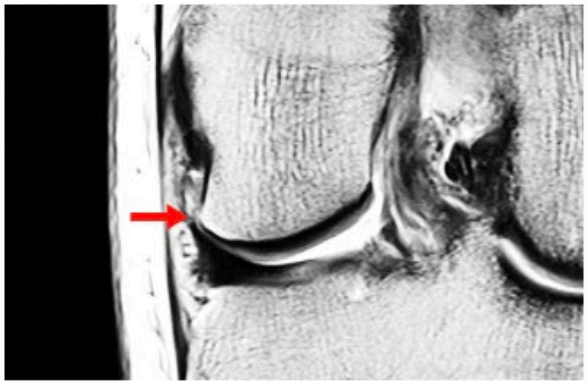

Medial Femoral Condyle

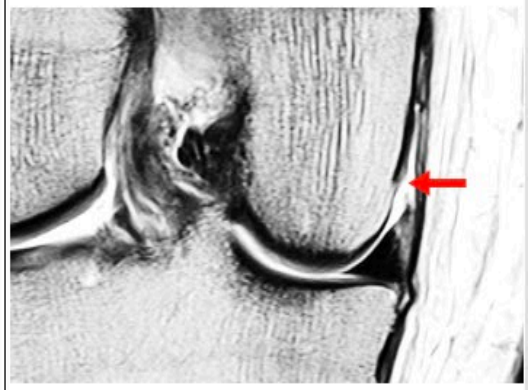

Trochlea

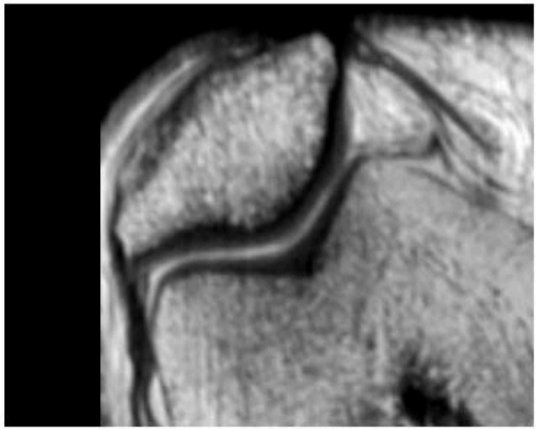

Lateral Tibial Plateau

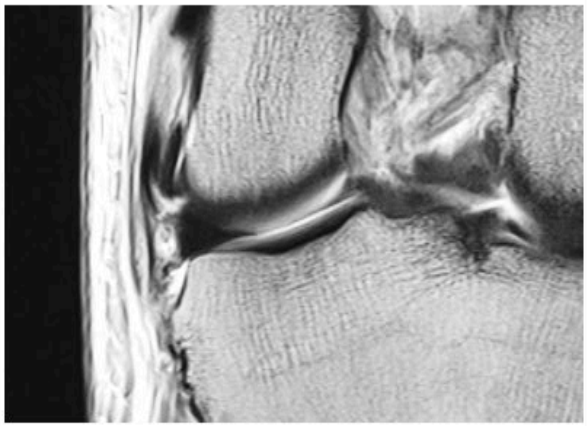

Medial Tibial Plateau

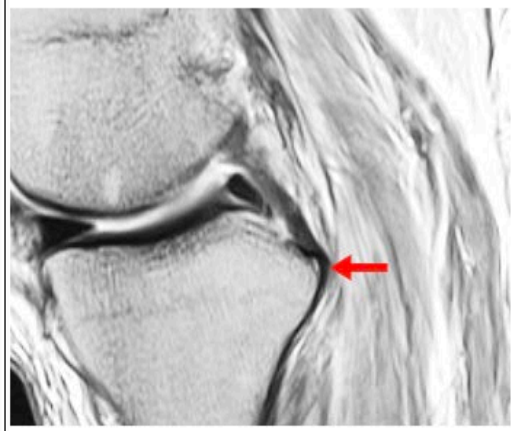

S2-RK

Meniscus: Severity

Anterior Horn - Lateral Meniscus

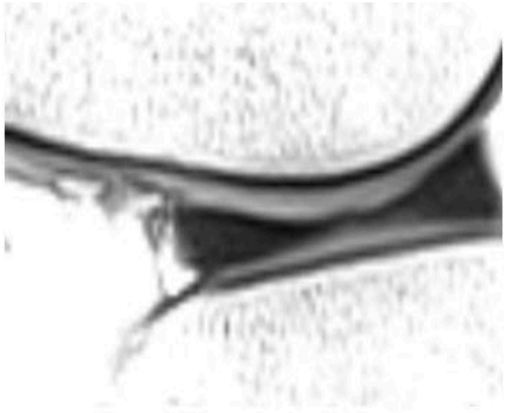

Body - Lateral Meniscus

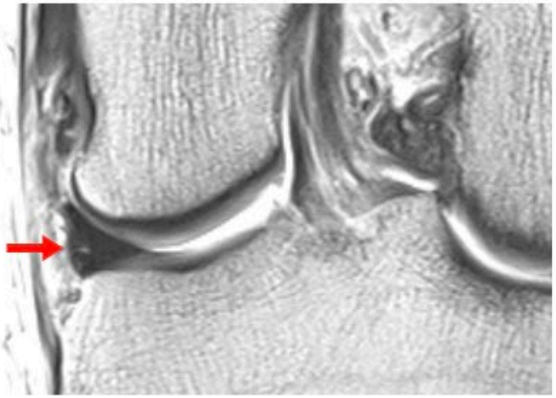

Posterior Horn - Lateral Meniscus

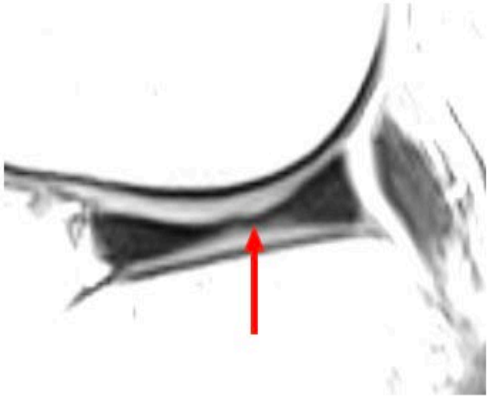

Anterior Horn - Medial Meniscus

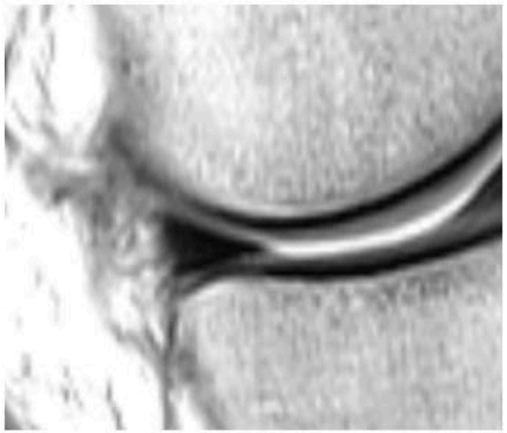

Body Medial Meniscus

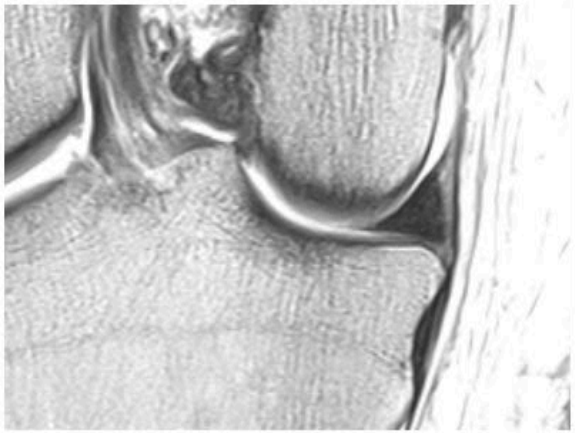

Posterior Horn - Medial Meniscus

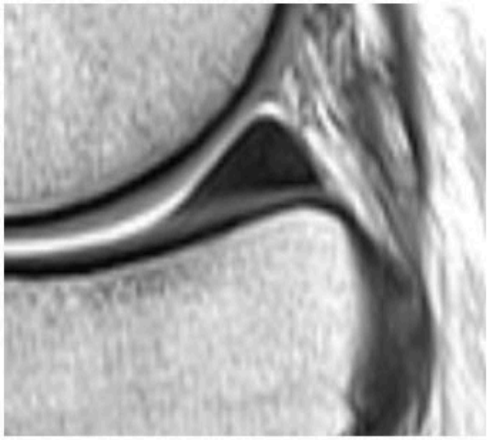

S2-RK

Ligaments

ACL

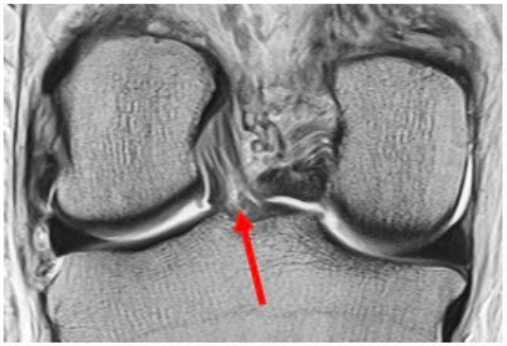

PCL

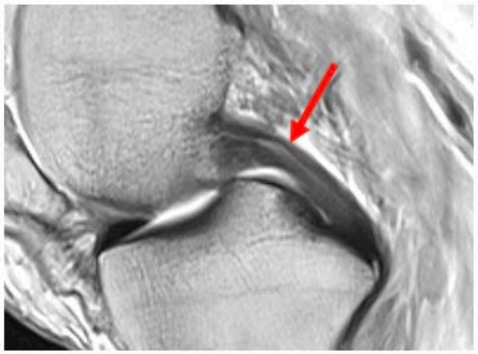

MCL

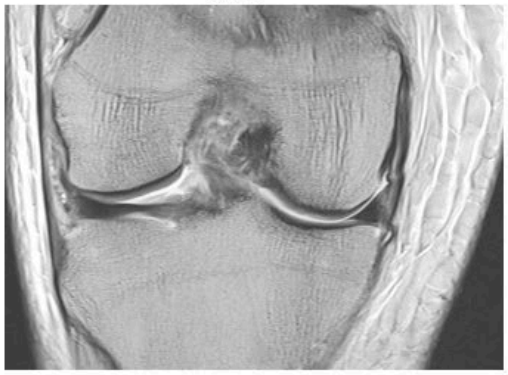

LCL

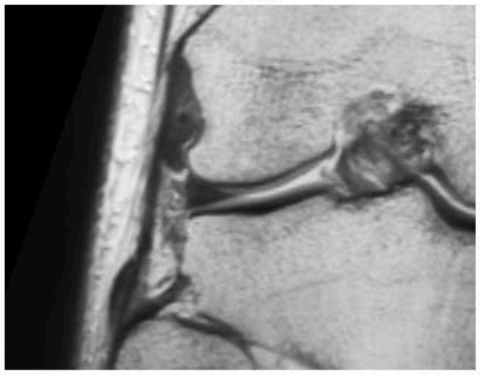

S2-RK

Synovitis / Fat Pad

Synovitis - Effusion

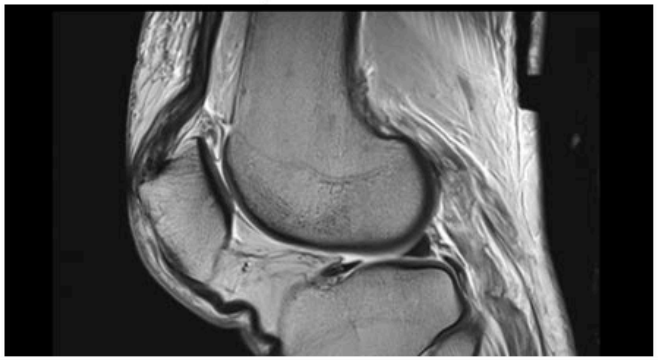

Pre femoral fat pad

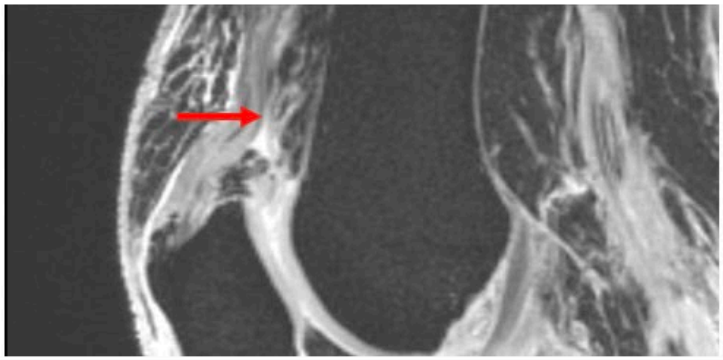

Supra patella fat pad

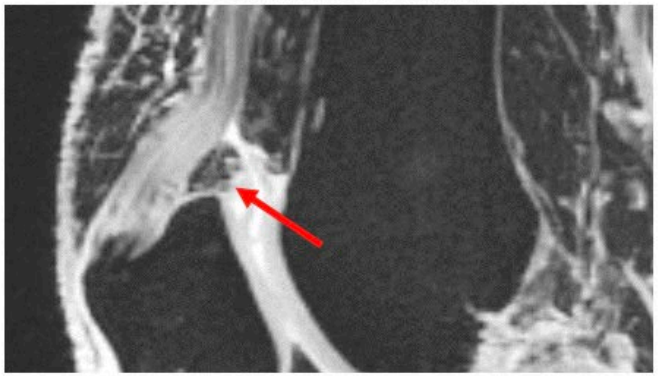

Hoffa's fat pad

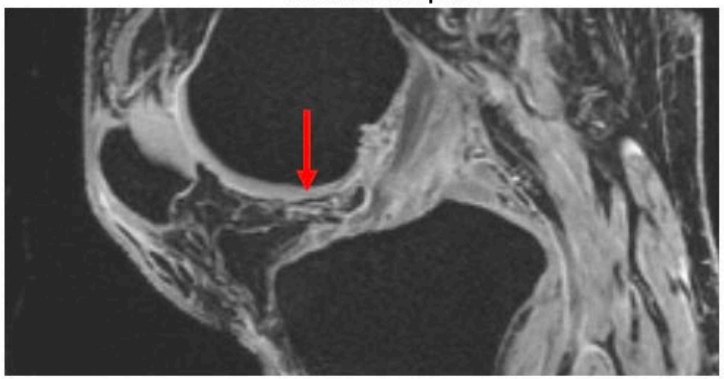

Appendix C: Subject 2 Left Knee MRI Images

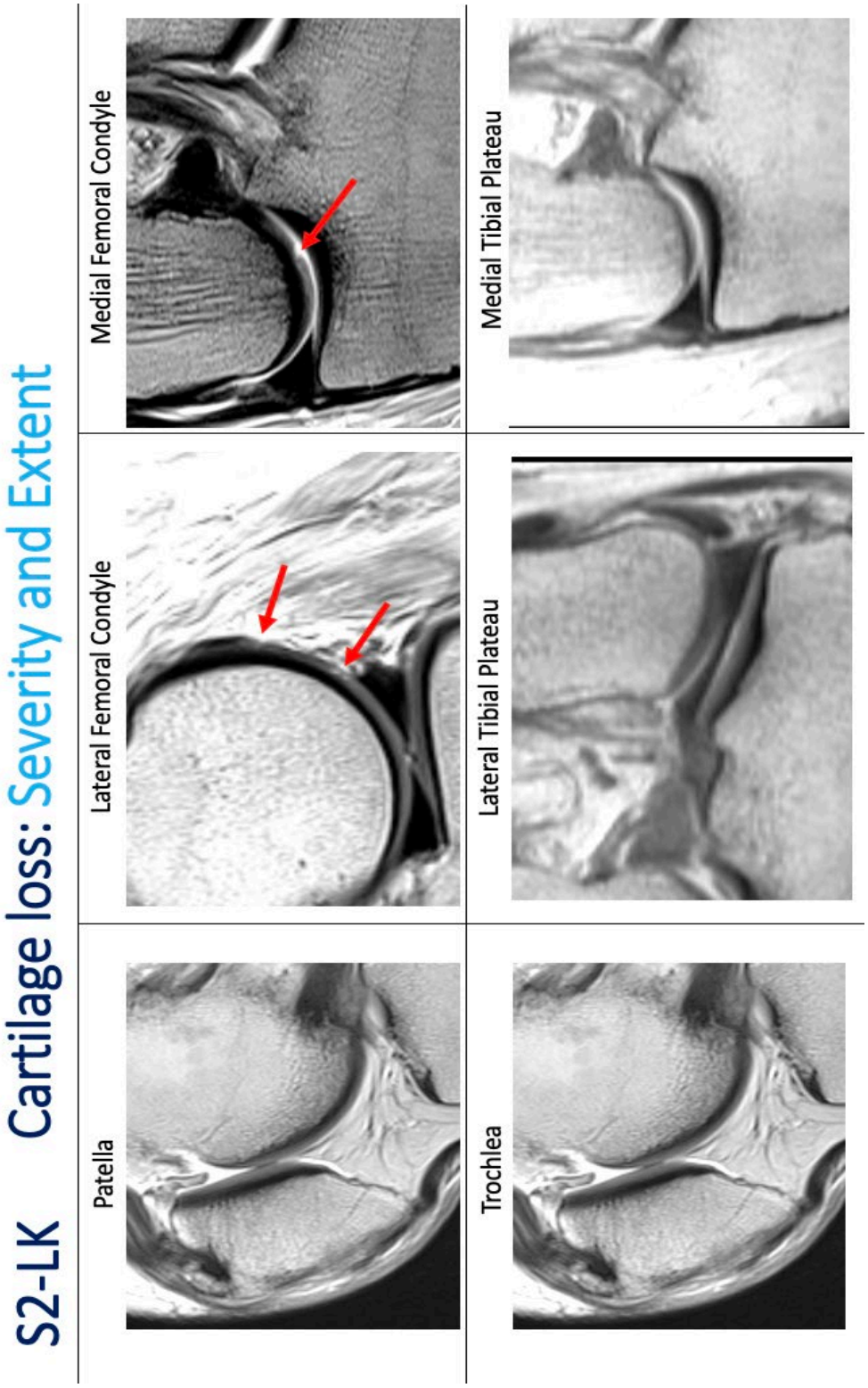

S2-LK

BME or Cyst

Patella

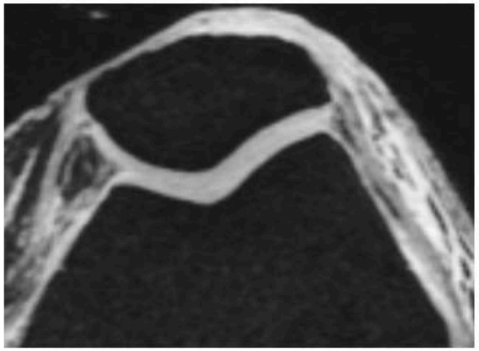

Lateral Femoral Condyle

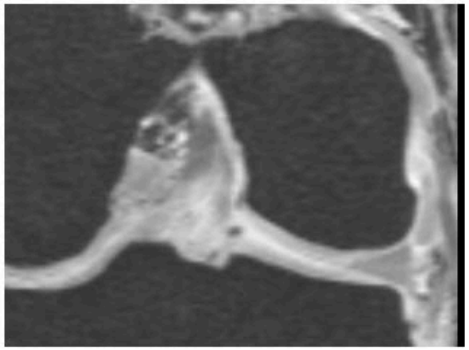

Medial Femoral Condyle

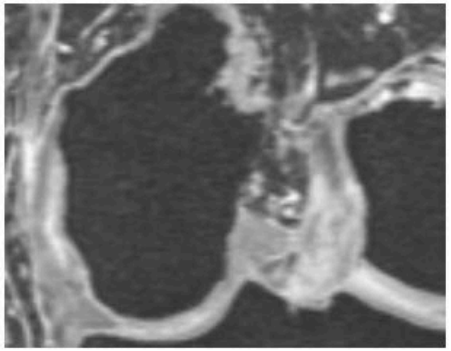

Trochlea

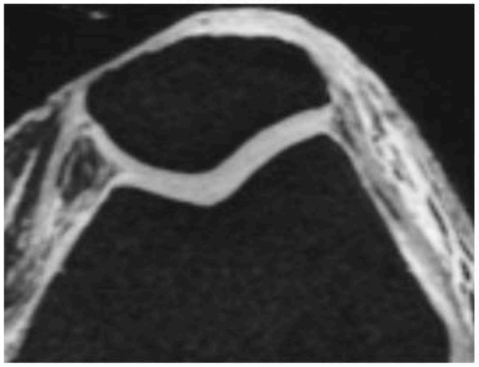

Lateral Tibial Plateau

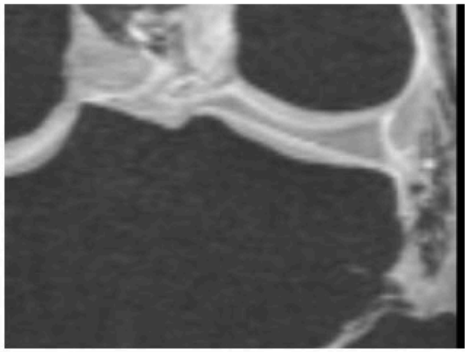

Medial Tibial Plateau

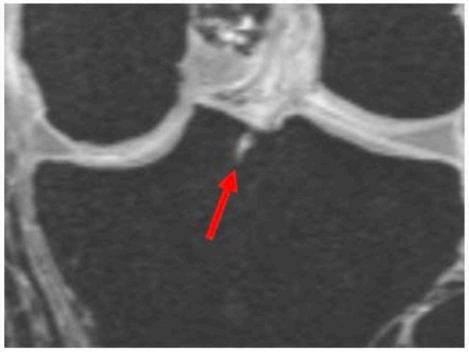

S2-LK

Osteophytes

Patella

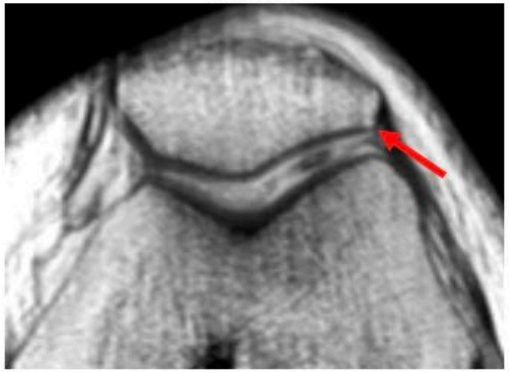

Lateral Femoral Condyle

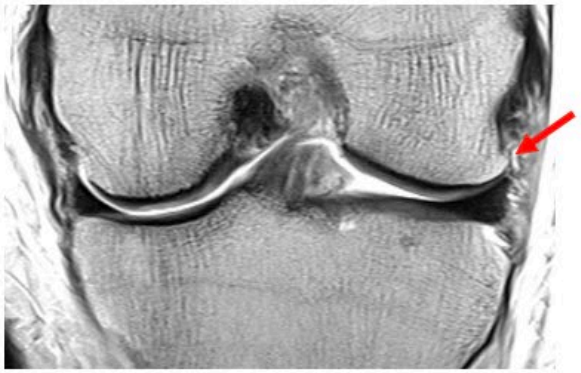

Medial Femoral Condyle

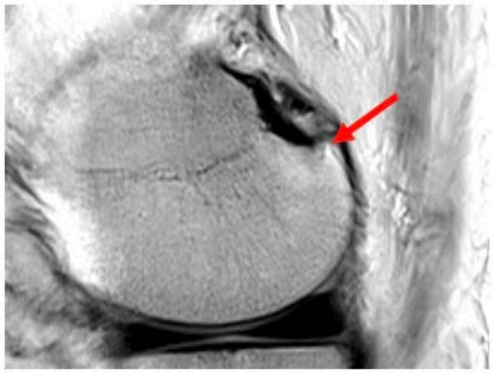

Trochlea

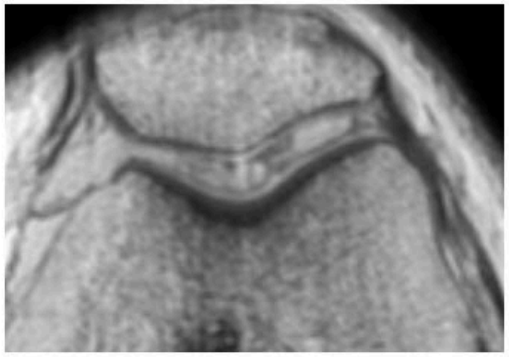

Lateral Tibial Plateau

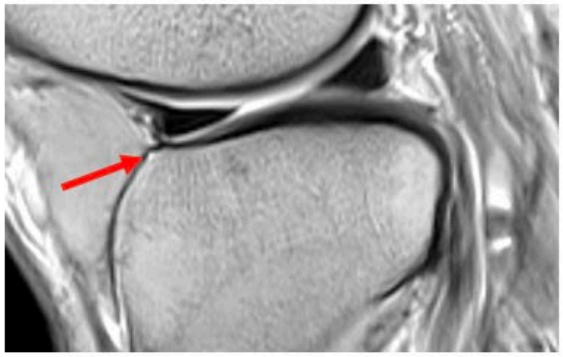

Medial Tibial Plateau

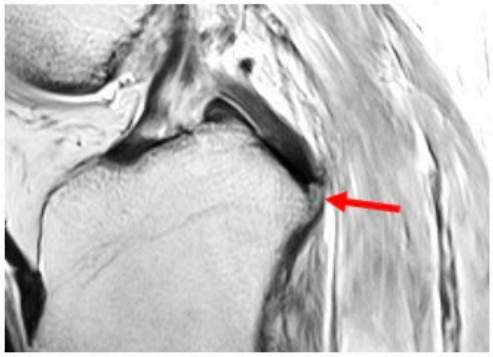

S2-LK

Meniscus: Severity

Anterior Horn - Lateral Meniscus

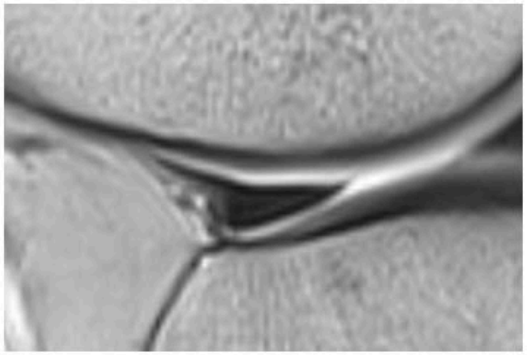

Body - Lateral Meniscus

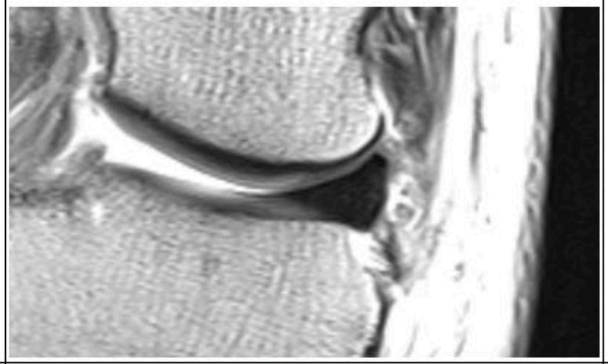

Posterior Horn - Lateral Meniscus

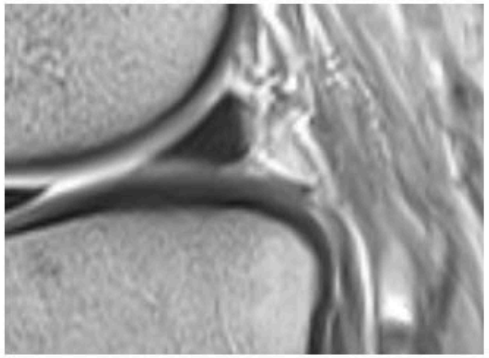

Anterior Horn - Medial Meniscus

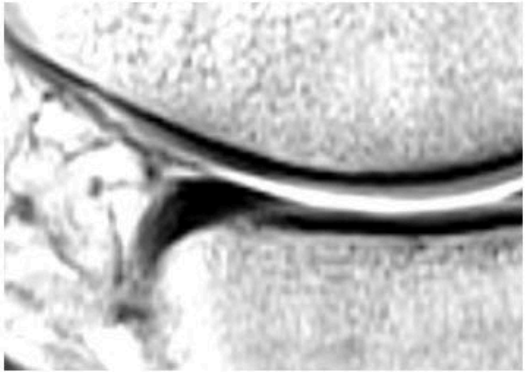

Body Medial Meniscus

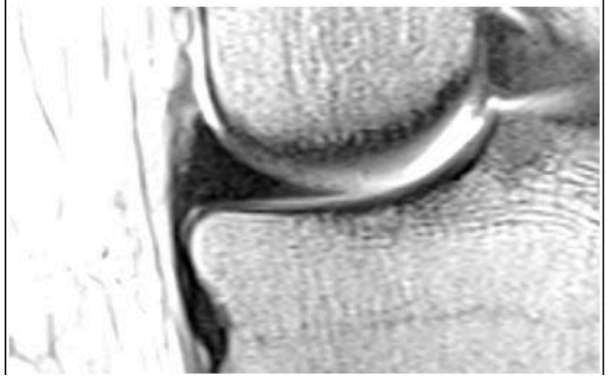

Posterior Horn - Medial Meniscus

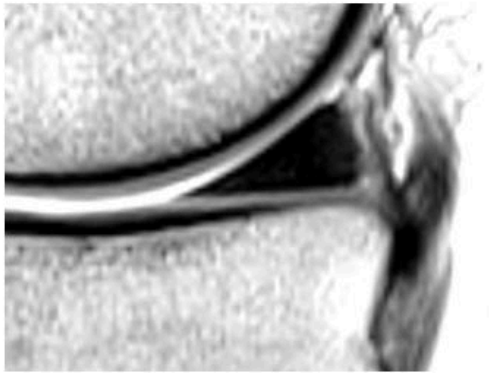

S2-LK

Ligaments

ACL

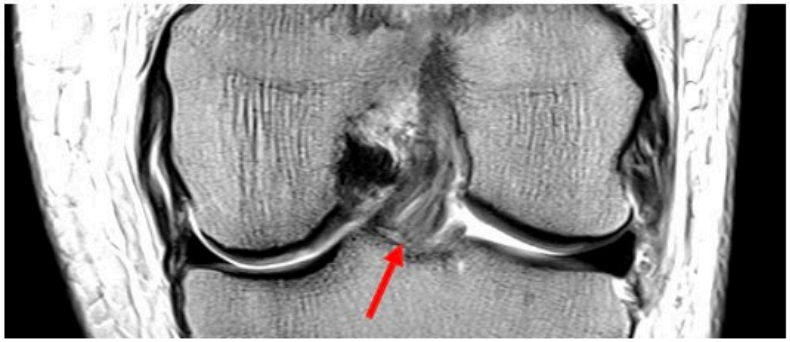

PCL

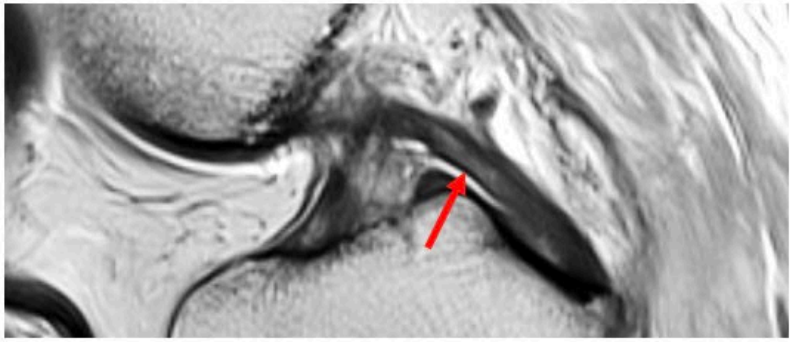

MCL

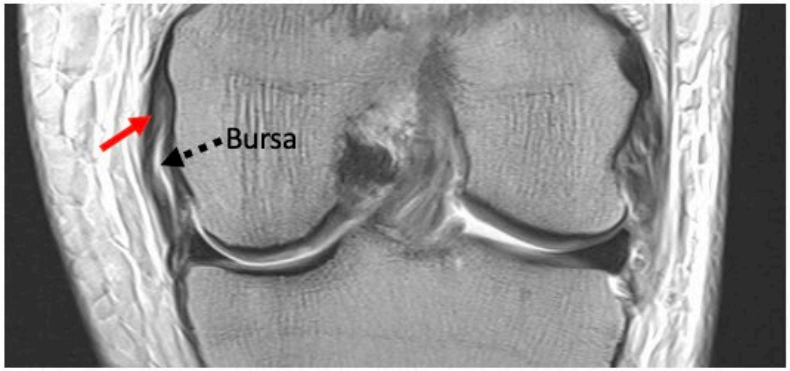

LCL

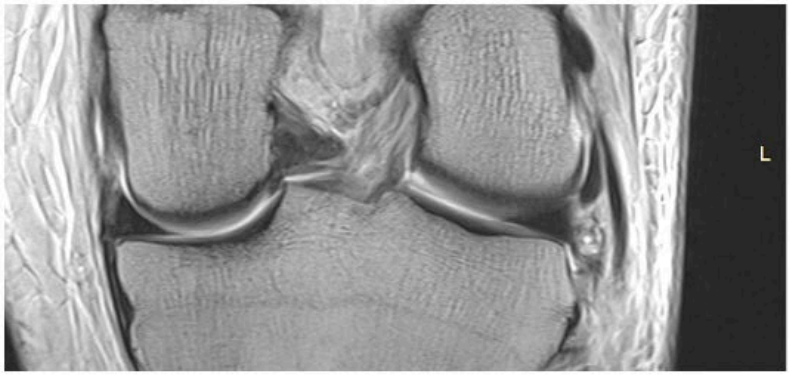

S2-LK

Synovitis / Fat Pad

Synovitis - Effusion

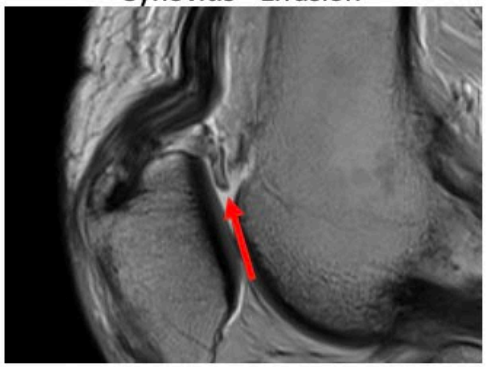

Pre femoral fat pad

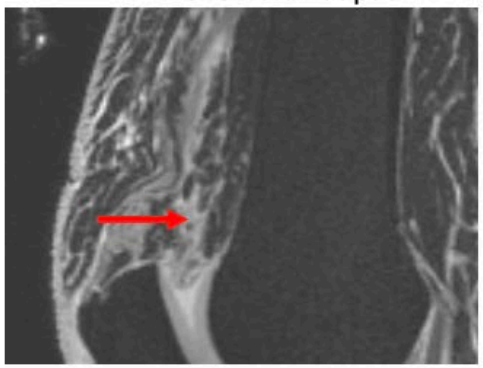

Supra patella fat pad

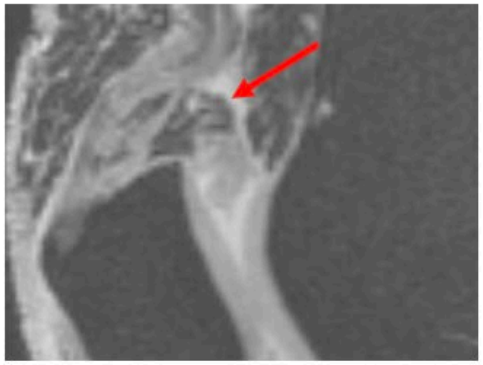

Hoffa's fat pad

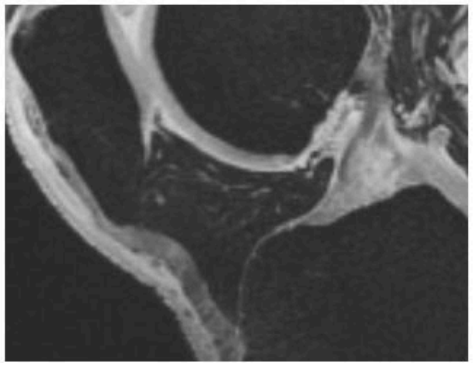

Bibliography

Ahmed, A. F., Azeem, A. A., Eladawy, A., & Abdeen, M. (2017, December 15). *MRI as an accurate tool for the diagnosis and characterization of different knee joint meniscal injuries*. The Egyptian Journal of Radiology and Nuclear Medicine. Retrieved November 12, 2021, from https://www.sciencedirect.com/science/article/pii/S0378603X17301286#b0055.

Bertrand, J. (2017). Role of Proteoglycans in Osteoarthritis. In A. Held (Ed.), *Cartilage* (Vol. 2, pp. 66–80). essay, Cham Springer.

Braun, H. J., & Gold, G. E. (2012, August). *Diagnosis of osteoarthritis: Imaging*. Bone. Retrieved November 12, 2021, from https://www.ncbi.nlm.nih.gov/pmc/articles/PMC3306456/.

Brody, L. T. (2015, November 16). *Knee osteoarthritis: Clinical connections to articular cartilage structure and function*. Physical therapy in sport : official journal of the Association of Chartered Physiotherapists in Sports Medicine. Retrieved November 12, 2021, from https://pubmed.ncbi.nlm.nih.gov/25783021/.m.

Buckwalter, J. A., & Mankin, H. J. (1998). *Articular cartilage: Degeneration and osteoarthritis, repair, regeneration, and transplantation*. Instructional course lectures. Retrieved November 12, 2021, from https://pubmed.ncbi.nlm.nih.gov/9571450/.

Centers for Disease Control and Prevention. (2020, July 27). *Osteoarthritis (OA)*. Centers for Disease Control and Prevention. Retrieved November 12, 2021, from https://www.cdc.gov/arthritis/basics/osteoarthritis.htm.

Culvenor, A. G., Øiestad, B. E., Hart, H. F., Stefanik, J. J., Guermazi, A., & Crossley, K. M. (2019, October 1). *Prevalence of knee osteoarthritis features on magnetic resonance imaging in asymptomatic uninjured adults: A systematic review and meta-analysis*. British Journal of Sports Medicine. Retrieved November 12, 2021, from https://bjsm.bmj.com/content/53/20/1268.

Foret, J. (2017, November 16). *Know your knees*. Center for Orthopaedics. Retrieved November 12, 2021, from https://www.centerfororthо.com/blog/know-your-knees/.

Guermazi, A., Niu, J., Hayashi, D., Roemer, F. W., Englund, M., Neogi, T., Aliabadi, P., McLennan, C. E., & Felson, D. T. (2012, August 29). *Prevalence of abnormalities in knees detected by MRI in adults without knee osteoarthritis: Population based observational study (Framingham osteoarthritis study)*. The BMJ. Retrieved November 12, 2021, from https://www.bmj.com/content/345/bmj.e5339.full.

Hayashi, D., Roemer, F. W., & Guermazi, A. (2019). *Magnetic Resonance Imaging Assessment of knee osteoarthritis: Current and developing new concepts and techniques*. Clinical and experimental rheumatology. Retrieved November 12, 2021, from https://pubmed.ncbi.nlm.nih.gov/31621571/.

Hsu, H., & Siwiec, R. M. (2021, July 25). *Knee osteoarthritis*. StatPearls [Internet]. Retrieved November 12, 2021, from https://www.ncbi.nlm.nih.gov/books/NBK507884/.

Jerban, S., Chang, E. Y., & Du, J. (2019, October 25). *Magnetic Resonance Imaging (MRI) studies of knee joint under mechanical loading: Review*. Magnetic Resonance Imaging. Retrieved November 12, 2021, from https://www.sciencedirect.com/science/article/pii/S0730725X19302887#bb0450 .

Katz, J. N., Arant, K. R., & Loeser, R. F. (2021, February 9). *Diagnosis and treatment of hip and knee osteoarthritis*. JAMA. Retrieved November 12, 2021, from https://jamanetwork.com/journals/jama/fullarticle/2776205.

Lyons, T. J., Stoddart, R. W., McClure, S. F., & McClure, J. (2005, March). *The tidemark of the chondro-osseous junction of the normal human knee joint*. Journal of molecular histology. Retrieved November 12, 2021, from https://pubmed.ncbi.nlm.nih.gov/15900412/.

Moore, K. H., Murphy, H. A., Chapman, H., & George, E. M. (2021, October 5). *Syncytialization alters the extracellular matrix and ...* American Journal of Physiology: Cell Physiology . Retrieved November 12, 2021, from https://journals.physiology.org/doi/full/10.1152/ajpcell.00177.2021.

Munoz-Garcia, N., Cordero-Ampuero, J., & Madero-Jarabo, R. (2020, August 7). *Diagnostic accuracy of magnetic resonance images and weight-bearing radiographs in patients with arthroscopic-proven medial osteoarthritis of the knee-nuria muñoz-garcía, José Cordero-Ampuero, Rosario Madero-Jarabo, 2020*. SAGE Journals. Retrieved November 12, 2021, from https://journals.sagepub.com/doi/10.1177/1179544120938369#bibr15-1179544120938369

Musumecci, G., Szychlinska, M. A., & Mobasheri, A. (2015, January 30). *Age-related degeneration of articular cartilage in the pathogenesis of osteoarthritis: Molecular markers of senescent chondrocytes*. Histology and histopathology. Retrieved November 12, 2021, from https://pubmed.ncbi.nlm.nih.gov/25010513/.

Peterfy, C., & Kothari, M. (2008, February 6). *Imaging osteoarthritis: Magnetic resonance imaging versus X-ray*. Current rheumatology reports. Retrieved November 12, 2021, from https://pubmed.ncbi.nlm.nih.gov/16515760/.

Roemer, F. W., Author AffiliationsFrom the Quantitative Imaging Center, DJ, H., GBD 2015 Disease and Injury Incidence and Prevalence Collaborators, T, V., Et Al., A, T., JW, B., N, A., JC, K., T, F.-B., JH, K., FW, R., A, G., MD, C., G, S., RD, A., U.S. Department of Health and Human Services Food and Drug Administration Center for Drug Evaluation and Research (CDER) Center for Biologics Evaluation and Research, PG, C., … Richardson, M. L. (2020, May 19). *State of the art: Imaging of osteoarthritis-revisited 2020*. Radiology. Retrieved November 12, 2021, from https://pubs.rsna.org/doi/full/10.1148/radiol.2020192498.

Sherman, S. L., Gulbrandsen, T. R., Lewis, H. A., Gregory, M. H., Capito, N. M., Gray, A. D., & Bal, B. S. (2018). *Overuse of magnetic resonance imaging in the diagnosis and treatment of moderate to severe osteoarthritis*. The Iowa orthopaedic journal. Retrieved November 12, 2021, from https://www.ncbi.nlm.nih.gov/pmc/articles/PMC6047403/.

Sophia Fox, A. J., Bedi, A., & Rodeo, S. A. (2009, November). *The basic science of articular cartilage: Structure, composition, and function*. Sports health. Retrieved November 12, 2021, from https://www.ncbi.nlm.nih.gov/pmc/articles/PMC3445147/.